**Title: The highly expressed lipid buffer FABP4 enforces adipocyte cell identity by driving the initial cell differentiation process**

**Authors:** Zahra Bahrami-Nejad[1,*], Tinghuan Chen[1,*], Stefan Tholen[1], Atefeh Rabiee[1], Michael L. Zhao[1], Ewa Bielczyk-Macynzka[1], Fredric B. Kraemer[2], and Mary N. Teruel[1,#]

**Affiliations:**
[1]Dept. of Chemical and Systems Biology, Stanford University, Stanford, CA
[2]Dept. of Medicine/Division of Endocrinology, Stanford University, Stanford, CA and VA Palo Alto Health Care System, Palo Alto, CA
*Equal Contribution

**#Corresponding Author:** mteruel@stanford.edu

## ABSTRACT

How differentiating progenitor cells can attain a distinct differentiated cell-identity is a challenging problem given the promiscuous nature of critical transcription factors and the typically fluctuating signaling environment in which cells exist. Here we test the hypothesis that a unique and robust differentiated cell identity can result from a core component of the differentiated state doubling up such that it has key functions in the differentiated state and also works at low levels as a positive-feedback signaling mediator that drives progenitor cells to differentiate. Using live single-cell fluorescence imaging analysis in the adipocyte differentiation system, we show that FABP4, one of the most abundant core components that buffers lipids in differentiated adipocytes, regulates at low levels expression of PPARG, the master regulator of adipocyte differentiation. Adipocyte progenitor cells transition from a priming phase of differentiation to a second phase during which low levels of FABP4 and PPARG mutually reinforce each other's expression. In this way both proteins reach a threshold where cells irreversibly commit to the differentiated state. Before and after reaching this threshold, PPARG transcriptionally increases FABP4 expression while fatty-acid loaded FABP4 binds to and increases PPARG activity. Together, our study suggests a control principle for robust cell identity, whereby a core component of the differentiated state also promotes differentiation from its own progenitor state.

## HIGHLIGHTS

- Only a small fraction (~10%) of the maximally reached FABP4 levels in cells is needed to commit cells to the differentiated state.
- Mature adipocytes express levels of FABP4 ten times the minimal level needed to commit cells to the differentiated state, thus providing an explanation for why the mature adipocyte state is so stable.
- Fatty-acid loaded FABP4 binds to and activates PPARG, thereby turning on PPARG positive feedback loops that increase PPARG expression.
- FABP4 critically controls the second phase of adipogenesis between activation of the feedback loops and reaching the threshold to differentiate.

## INTRODUCTION

Progenitor cells typically have the capacity to differentiate into two or more different cell types and cell differentiation itself can be plastic, with cells able to lose or change their differentiated state under some physiological and pathological conditions. Here we focus on a key open question of how cells can robustly attain a specific differentiated cell identity since most signaling elements and transcription factors that mediate differentiation are not unique to a specific differentiated state. As one mechanism supporting cell identity, negative feedback has been shown to play a role in regulating the differentiation decision between two fates whereby one fate can suppress the program that drives differentiation of the other fate [1]. Since this negative feedback mechanism mostly prevents cells which have chosen one path from differentiating into alternative cell types, additional regulatory mechanisms must exist that selectively drive cells onto a unique path and allow cells to robustly assume and maintain a specific differentiated cell identity. Positive feedback has been shown to be one such mechanisms that can help cells attain a unique cell identity by triggering one-way cell fate decisions that transition progenitor cells to a differentiated state. To generate an irreversible switch, at least one arm of the positive feedback has to be cooperative or ultrasensitive to generate bistability with strong hysteresis [2]. Furthermore, irreversible switches are made more robust when multiple parallel positive feedbacks engage [3]. Thus, a combination of ultra sensitivity and multiple positive feedbacks can create a bistable switch between two cell fates, that, if sufficiently strong, can generate unidirectional irreversibility which is ideally needed for an irreversible cell differentiation process [4–6]. Nevertheless, given the overlapping uses of signaling and transcription programs and the significant signaling variability between individual cells in a population, it is unclear how cells can navigate the signaling and transcriptional landscape in progenitor states and can be reliably directed towards the correct path that leads to a unique identity of the differentiated state.

Here we considered that one mechanism that could allow cells to assume a robust cell identity is a type of positive feedback whereby a core component that is uniquely expressed and needed in the differentiated state doubles-up by being also a signaling co-factor that is needed to drive the

differentiation decision (Fig 1A). Two requirements for an ideal cell-identity positive feedback are that it should (1) generate a delay before commitment to ensure that cells can select the correct differentiation path and cell identity and (2) once cells have committed, to robustly lock the cell into its differentiated cell identity. To test if such a positive-feedback mechanism exists and how it may reinforce cell identity of a differentiated state, we used the adipocyte cell differentiation system since it is a well-characterized and experimentally accessible terminal cell differentiation process. We were also intrigued by a previous observation that increased levels of fatty acids can promote differentiation of precursor cells. As a candidate for such a self-reinforcing mechanism for cell identity, the fatty acid binding protein, FAPB4, is highly abundant only in terminally differentiated adipocytes, where it makes up between 1-3% of soluble protein [7]. FABP4 is a critical core component that has important cell-internal functions in mature adipocytes such as binding to hormone sensitive lipase (HSL) and buffering lipid release [8]. However, there is also evidence that FABP4 has an additional role in positively regulating the transition from progenitor cells to mature adipocytes [9–11]. These observations motivated our study here that FABP4 could provide such a self-reinforcement mechanism for unique cell identity. Notably, FABP4 can be released from mature adipocytes and has cell-external roles in different cell types including preadipocytes and other adipocytes where it has been shown to reduce PPARG expression as a pathological and possibly also normal regulatory function [12].

In its cell-internal role, FABP4 is well-established as a downstream target of PPARG, the master regulator of adipocyte differentiation [13]. The other role of FABP4 in also regulating PPARG activity is less well understood. A recent study by our group provided one clue by showing that FABP4 mRNA has a long half-life which helps to reduce excessive adipogenesis under normal conditions where adipogenic hormones oscillate [11]. Nevertheless, key questions about the role of FABP4 in differentiation remain open as very little FABP4 is expressed early in adipogenesis. It is not clear how FABP4 regulates PPARG and if and how FABP4 and PPARG may reinforce each other's expression. Finally, if FABP4 is indeed uniquely important for adipogenesis, it is not clear why genetic studies in

FABP4-knockout mice failed to show a suppression of adipogenesis [14].

Here, using live single-cell analysis of endogenously-tagged PPARG and FABP4, we show that FABP4 and PPARG build up only very slowly during a first phase of the adipogenic program until they transition to a second phase marked by engagement of positive feedback between each other. This feedback starts after about 24 hours when the FABP4 level is very low and ends approximately 12 hours later when the levels of PPARG and FABP4 rapidly build up and pass a critical threshold for differentiation. Despite the low level of FABP4 at this time, we show that the feedback-activation of PPARG can be repressed by a mutant FABP4 that is deficient in binding fatty acid. Since we also found a direct interaction of FABP4 with PPARG, our study can best be interpreted by FABP4 having already at low levels a transport function to enhance fatty acid binding to PPARG, a mechanism which is known to increase PPARG activity [13]. We also provide evidence that upregulated FABP5, upon ablation of FABP4, can explain the previously observed lack of an effect on differentiation in FABP4-knockout mice, which is in-line with studies showing that FABP5 compensates for FABP4 in FABP4-knockout mice [15]. Together, our study provides support for a general model that robust cell identity can be initiated and reinforced by having a unique core component of the differentiated state double-up as a signaling factor that initiates and reinforces the path to a unique differentiated state.

## RESULTS

### FABP4 is needed for adipogenesis in vitro and in vivo

Previous studies support that FABP4 and PPARG are in a positive feedback relationship [9,11,16,17]. One arm of this positive feedback is well-established since there are PPARG binding sites on the FABP4 promoter, and PPARG activity has been shown to strongly upregulate FABP4 mRNA and protein levels [7]. However, the relevance of FABP4 in regulating PPARG has been controversial as FABP4 knockout mice were not defective in adipogenesis [14]. We therefore performed a series of experiments to address if and how FABP4 can regulate PPARG expression and adipogenesis. Using the adipogenesis assay described in Fig 1B, we first carried out shRNA-mediated

depletion of FABP4 in the OP9 preadipocyte system and induced adipogenesis with the standard DMI protocol. We observed that FABP4 knockdown partially reduced adipogenesis (Fig 1C). We also knocked down FABP5 since studies have shown that FABP5 is upregulated when FAP4 is ablated and may be able to compensate for the loss of FABP4. Knockdown of FABP5 and FABP4 further reduced adipogenesis compared to knockout of FABP4 alone but adipogenesis was not completely suppressed.

Since we observed significant adipogenesis in the dual shRNA knockdown experiments, we thought this might be due to the fact that endogenous FABP4 is highly expressed during adipogenesis, and thus FABP4 levels might be too high to obtain efficient knockdown. To remove all endogenous FABP4 from the cells, we used CRISPR-mediated genome editing to completely knock out FABP4 expression in OP9 cells (Fig 1D). We then induced differentiation using the standard DMI protocol. As expected, control-KO OP9 cells differentiated robustly (Fig 1E). In contrast, FABP4-KO OP9 cells were strongly defective in increasing PPARG expression and differentiating, with less than 10% of cells differentiating compared to control cells. Since FABP5 has been shown to compensate for FABP4 knock-out both in vitro and in vivo [14,15,18], we also tested whether we could further reduce the amount of adipogenesis in the FABP4-KO cells by also knocking down FABP5 using siRNA. Indeed, we could reduce adipogenesis to almost nothing when we knocked down both FABP4 and FABP5.

We further validated these findings in another commonly used preadipocyte cell system, 3T3-F442A cells [19]. We used CRISPR-mediated genome editing to knockout FABP4, FABP5, or both FABP4 and FABP5 (Fig 1F). 3T3-F442A cells which had been subjected to the same FABP4 knockout protocol but which did not harbor any FABP4 knockout were used as control cells. We plated the 3T3-F442A cells into 96-well plates and induced adipogenesis using the standard protocol in 3T3-F442A cells which is to add insulin[19]. Indeed, when FABP4 or FABP5 or both were knocked out, 3T3-F442A preadipocytes showed reduced differentiation, as measured by PPARG staining, as well as lipid accumulation, as measured by Oil Red-O staining (Fig 1G and 1H). The latter is indicative that the KO cells are not functional mature adipocytes. To test whether FABP4 was essential for adipogenesis in

vivo, we used a previously-established method in which 3T3-F442A preadipocytes are subcutaneously injected into the sternum of immune-deficient mice, giving rise to fat pads resembling normal adipose tissue[20]. Since fat is not normally present at the sterum of mice, the fat pad formed at the sterum after injection of preadipocyte cells is generated by de novo adipogenesis of the injected cells[20]. We injected our preadipocyte cells into the sterum of 8-week mice, and a fat pad was allowed to form for 4 weeks. The FABP4-KO, FABP5-KO, and DBKO preadipocyte cells indeed showed a defect in adipogenesis, as measured by weighing the fat that formed at the sternum (Fig 1I, 1J, and S1). Taken together, we conclude that FABP4 and its homolog FABP5 have a critical role in mediating adipogenesis in vitro and in vivo.

**Overexpression of FABP4 in drives differentiation of preadipocytes, as well as mescenchymal stem cells (MSCs), into adipocytes**

The role of FABP4 has been controversial, and thus as shown in the results in Figure 1, we had used FABP4 knockout or knockdown experiments both in vitro and in vivo to demonstrate that FABP4 could regulate PPARG expression and adipogenesis. We now wanted to test whether overexpression of FABP4 would have the converse effects on PPARG expression and adipogenesis as the FABP4 knockdown and knockout experiments. We thus introduced doxycycline-inducible YFP-FABP4 or YFP(control) constructs into OP9 cells but saw no difference in their effect on adipogenesis (Fig 2A). We speculated that this lack of a difference was due to the fact that FABP4 is so highly expressed during adipogenesis that overexpression of FABP4 would have little effect on top of the endogeneous FABP4. We thus took advantage of our FABP4-KO preadipocyte cell line (Fig 1B). We made stable FABP4-KO cells expressing doxycycline-inducible YFP-FABP4 or YFP(control) (Fig 2B). Indeed in the background of no endogeneous FABP4, it was apparent that overexpression of FABP4 could rescue differentiation capacity (Fig 2C).

To determine whether inducing FABP4 alone is sufficient to commit mesenchymal stem cells into adipocytes, we used C3H10T1/2 cells, a well established mesenchymal stem cell (MSC) model

which is capable of differentiating into different cell fates. We used a C3H10T1/2 MSC line that was stably expressing the two core components of the SAM system (C3H/10T1/2-CRISPRa-SAM [21]) and transfected sgRNA targeting the promoter regions of the FABP4 to induce FABP4 expression 2 days before we differentiated the cells (Fig 2D). Induction of FABP4 increased PPARG expression and the number of mature adipocytes (Fig 2E).Taken together, our results suggest that FABP4 expression can increase PPARG expression and that FABP4 expression is sufficient to commit preadipocytes and MSCs into becoming mature adipocytes.

**CRISPR-mediated genome editing and live-cell imaging shows very small but significant increase in FABP4 levels before cells reach the threshold for differentiation**

Previous in vitro work [3,17,22] and our in vitro and in vivo results (Fig 1) argue that PPARG not only increases FABP4 expression but that FABP4 also increases PPARG expression and adipocyte differentiation. To understand when and how this positive feedback between PPARG and FABP4 can engage during the multi-day differentiation process, we carried out live-cell imaging experiments to determine precisely when FABP4 and PPARG increase relative to each other in the same single cells. We first used CRISPR-mediated genome editing to tag endogenous FABP4 and PPARG in mouse OP9 preadipocyte cells with orthogonal fluorescent proteins (Figures 3A, S1, S2). Using these dual-tagged (YFP)-PPARG and mKate2(RFP)-FABP4 cells, we carried out time-course analysis in thousands of individual cells while applying a 48-hour long adipogenic (DMI) stimulus. As shown in Fig 3B, changes in PPARG and FABP4 levels showed an overall similar dynamic over the four-day timecourse of adipogenesis. However, the individual time-course traces showed significant cell-to-cell variability. To better understand how PPARG and FABP4 protein levels change with respect to each other in the same cell, we compared PPARG and FABP4 timecourses in individual cells (Fig 3C). Both protein levels increased very slowly for the first 24 hours before increasing more rapidly from 24-48 hours and then further increasing their respective abundances for days even after DMI removal.

Nevertheless, even though PPARG and FABP4 protein expression dynamics looked similar, the relative increase in the levels of PPARG and FABP4 was significantly different during the time course (Fig 3D). Note that the axis for the FABP4, but not of the PPARG, signal in Fig 2C is logarithmic in order to better visualize the relatively small early increase in FABP4 in the first 48 hours. While PPARG levels increased steadily over the time-course of adipogenesis, reaching approximately 20% of maximal by 24 hours and approximately 45% of maximal by 48 hours, the increase in FABP4 had a markedly different behavior (Fig 3E). FABP4 increased steadily, but it only by a few percent of maximal in the first 24 hours and then to only 10% of maximal by 48 hours. This very small early increase in FABP4 is hard to see without quantitative timecourse imaging such as in the current study or without quantitative proteomics which also observed the same small early FABP4 increase [3]. Previous studies using approaches such as Western blots to quantify FABP4 expression during adipogenesis lacked the sensitivity to observe the small early FABP4 increase that occurs only in the subset of cells that differentiate which is likely the reason why it has been commonly thought that FABP4 is only downstream of PPARG and is induced late in adipogenesis after the critical signaling events for differentiation have already happened.

**FABP4 is not needed early in adipogenesis, but is needed later to reach the threshold at which cells irreversibly commit to differentiate**

Our results so far support previous work which showed that FABP4 is in a positive feedback with PPARG [9,16,17]. In the widely-accepted model of adipocyte differentiation, cell-intrinsic positive feedback to PPARG (Fig 4A) must engage for cells to irreversibly differentiate. As shown in Fig 4B, in cells that have reached the PPARG threshold, PPARG levels are able to continue to increase and the cells do not fall back to the undifferentiated state even after the external stimulus is removed[23–25]. Upon addition of the adipogenic DMI stimulus, PPARG levels increase both in response to the stimulus and because of positive feedback (Fig 4A). This raises the question when the positive feedback engages in a particular cell. When inspecting individual traces before DMI is removed (Fig 4C), one

can distinguish a transition from a first Phase during which PPARG abundance linearly increases at a slow rate (shallow slope) to a second Phase during which PPARG increases at a much faster rate (slope steepens). An analysis of averaged single cell traces in Fig 4D shows that the shallow slope lasts for approximately 24 hours (dotted black line marked “1”) before the slope becomes gradually steeper between 24 to 48 hours (dotted black lines marked 2-5). When plotting the slope of PPARG as a function of time, the two phases can be more clearly distinguished (Fig 4E). It is plausible that the relatively constant increase in PPARG abundance in Phase 1 reflects the cell’s initial response to the external DMI stimulus, while the accelerated increase in the slope of PPARG after approximately 24 hours of DMI stimulation reflects the start of the induction of cell-intrinsic positive feedbacks that amplify PPARG expression. In strong support of this model, this second Phase is absent in cells in which CEBPA and FABP4, both positive feedback regulators of PPARG, are depleted (Fig 4F and 4G), arguing that the accelerated increase in the slope of PPARG is a direct measure of when the positive feedback starts to engage. We therefore termed the clear transition between Phases 1 and 2 the "feedback engagement point". Knocking down CEBPB suppresses the initial gradual PPARG increase (Fig 4H), supporting that, in contrast to FABP4 and CEBPA, CEBPB is needed very early in adipogenesis to increase PPARG levels to the feedback engagement point.

The timecourses in Figures 4B and 4C show that the feedback engagement point occurs long before the threshold is reached, arguing that differentiation cannot occur unless the cell-intrinsic positive feedback engages and has time to become strong enough to keep increasing PPARG levels independently of the external differentiation (DMI) stimulus. PPARG abundance has been shown to be predictive of differentiation outcome [11,26], but to determine whether the slope of PPARG could also predict differentiation outcome, we calculated and compared histograms of the abundance and slope of PPARG in cells at 44 hours before DMI removal. As shown in Fig 4I, differentiation outcome can be predicted equally well, or even better, if the threshold is calculated using PPARG slope instead of PPARG abundance (accuracy of prediction is 94% using slope versus 90% using abundance). The fact that a high slope of PPARG, which requires engagement of positive feedback, is highly predictive

of the differentiation outcome suggests that the strength of cell-intrinsic feedback to PPARG determines whether or not the irreversible differentiation switch will be triggered when DMI is removed.

**An early small increase in FABP4 upregulates PPARG expression before cells reach the threshold to differentiate**

To better understand the significance of the early small increase in FABP4 concentration during differentiation observed in Figures 3D and 3E, we performed a detailed analysis of the respective increases of PPARG and FABP4 before cells reach the critical threshold, typically around 24-36 hours after inducing differentiation. Such a single-cell analysis is relevant since the respective increases show a large degree of variability between individual cells in the same population. As shown in the example timecourses of hundreds of cells in Fig 3B, there appears to be a close correlation in the kinetics when PPARG and FABP4 increases: Cells that increase PPARG early also ramp up FABP4 earlier. This correlation becomes clearer when separating cells into 3 bins based on when they upregulated PPARG after inducing differentiation and plotting the average of the bins (Fig 5A). The close correlation between the respective PPARG and FABP4 increases is apparent. Zooming in closer on the the first 36 hours (Fig 5B) shows that PPARG levels start to ramp up at different times from 18 to 36 hours and FABP4 also starts to ramp up in each case at the same time. The coincidence of the increase in PPARG and FABP4 is consistent with PPARG regulating FABP4 and also supports a previous hypothesis that FABP4 and PPARG are connected by positive feedback [11,27]

A logarithmic comparison of the averaged signals in cells that will differentiate (Fig 5A, red line) versus cells that will not (Fig 5C, black line) shows that the feedback engagement point when the slope starts to increase is several hours before the threshold for differentiation. Furthermore, in cells that will not reach the PPARG threshold when DMI is removed, PPARG levels raise more slowly from the start compared to cells that will differentiate. In addition, PPARG will again gradually drop after DMI is removed in cells that fail to differentiate. For FABP4, the intial increase is not distinguishable

between cells that differentiate or not, suggesting that FABP4 becomes mostly rate-liming at the engagement point where FAPP4 starts to increase along with PPARG.

Together with the siRNA data shown in Fig 4F-H, these results are consistent with the interpretation that CEBPB drives the initial slow gradual increase in PPARG and that positive feedback between PPARG and CEBPA, as well as positive feedback between PPARG and FABP4, both drive parallel increases in the proteins that starts at the feedback engagement point and raises PPARG levels for another 12-24 hours to reach above the threshold for differentiation (Fig 5D). This data argues that terminal cell differentiation can be described as a three-phase process marked by whether the PPARG increase is primarily driven externally by the differentiation stimulus (Phase 1), cell-intrinsically by the positive feedbacks (Phase 3), or both during the time window in between (Phase 2). Of note, the threshold, which marks the transition between Phase 2 and Phase 3, is not visible from inspecting the single-cell or averaged traces and needs to be identified by using live-cell imaging to measure PPARG levels before removing the external differentiation stimulus and then continuing to track each individual cell to know their final differentiation state days later. Thus, the time-course of differentiation can be broken into an early linear phase and a middle phase where FABP4 reinforces PPARG activity or expression so that cells can reach a critical threshold when differentiation becomes permanent.

**FABP4 needs to transport lipid ligand to PPARG in order for preadipocytes to differentiate**

Data from the literature suggested that FABP4 may have a role inside cells to deliver fatty-acid ligands from the cytosol to the nuclear receptor PPARG [9], thereby enhancing the transcriptional activity of PPARG. Since such a role of FABP4 has been controversial, we took advantage of our knockout cell line to test whether the transcriptional activity of PPARG is indeed enhanced by FABP4 being able to transport lipid ligand to PPARG. We also made use of previous work which showed that an R126Q mutation in FABP4 results in a 30-50-fold reduction in the binding affinity for long chain fatty acids (Fig 6A) [28]. When expressing this fatty-acid binding deficient construct in control cells, we

already observed a 30% suppression of differentiation, suggesting that the construct may have a dominant negative effect (Fig 6B). We next made stable FABP4-KO OP9 cell lines with doxycycline-inducible YFP-FABP4, YFP-FABP4(R126Q) non-fatty acid binding mutant, or YFP(control) (Fig 6B). Introducing wildtype FABP4 into FABP4-KO cells rescued the differentiation capacity (Fig 6C). In contrast, FABP4-KO cells in which FABP4-R126Q, a non-fatty acid binding mutant of FABP4, was expressed resulted not only in no differentiation, but PPARG levels dropped even below control levels, further suggesting that the mutant FABP4 can suppress PPARG in a dominant-negative manner (Fig 6C).

To determine whether FABP4's ability to transport lipid is needed to activate PPARG, we introduced a PPARG-responsive reporter, PPRE3-mKate2-NLS-PEST, consisting of three repeats of a PPRE promoter sequence to which PPARG has been shown to bind (Fig 6D) [29]. The 3X-PPRE sequence was fused to a mKate2 (RFP) fluorescent protein and to a PEST domain of ornithine decarboxylase sequence to destabilize the mKate2 fusion and therefore ensure that the sensor could also measure down regulation of promoter activity. Also, a nuclear localization signal (NLS) was added to ensure that the mKate2 fluorescent signal is restricted to the cell nucleus, which results in better segmentation for time-course analysis.

As shown in Fig 6E, expression of YFP-WT-FABP4 and subsequent addition of linoleic acid, a naturally occurring PPARG ligand [22] and one of the predominant fatty acids of adipocytes [30], resulted in higher induction of PPRE activity compared to expression of YFP as a control. These results suggest that FABP4 activates PPARG in a ligand-dependent manner. Importantly, expression of the mutant FABP4 that could not bind lipid resulted in a significant reduction in PPARG activity compared to expression of YFP. This result is consistent with the effects that we observed for this same mutant on adipogenesis. Together, the ability of WT-FABP4, but not mutant-FABP4, to selectively promote PPARG activity supports that the lipid transport capability of FABP4 promotes PPARG activation.

If FABP4 transports lipids to PPARG, the two proteins should directly interact. To test whether FABP4 and PPARG directly interact, we overexpressed YFP-FABP4, YFP-FABP4-mutant, or YFP(control) in OP9 cells and performed a co-immunoprecipitation (coIP) assay using a GFP-nanobody (Fig 6F). We found that FABP4 and PPARG indeed interact in a lipid-dependent manner, suggesting that lipid-loaded FABP4 can directly transfer lipid to PPARG. Interestingly, we found that the fatty-acid binding deficient mutant-FABP4 is bound to PPARG regardless of whether fatty acid was present or not, explaining the observed dominant negative effect.

**Rosiglitazone is a small molecule that can directly bind to the PPARG lipid binding pocket without requiring FABP4**

Given the results thus far, there is a puzzling finding in the literature that FABP4/5 deficient precursor cells can still differentiate into adipocytes upon treatment with rosiglitazone, a small molecule activator of PPARG. We were indeed able to reproduce this results in the 3T3-F442A knockout FABP4 and knockout FABP4/5 cell models. Fig 7A shows that rosiglitazone can restore all of the differentiation in the single knockout and approximately 50% of the differentiation in double knockout cells compared to control cells. Fig 7B shows the same analysis for the single and double knockout OP9 cell model with an even higher fraction of differentiation being restored. A live-cell analysis of rosiglitazone addition in cells with endogenously tagged PPARG provides mechanistic insights how rosiglitazone acts. In DMI-stimulated control cells, addition of rosiglitazone has little effect early in adipogenesis but then causes a much more rapid increase in PPARG levels when the feedback engagement point is reached after 24-36 hours (Fig 7C). For the same conditions with and without rosiglitazone, FABP4 or FABP4/5 knockdown suppresses the rapid increase in control cells. However, rosiglitazone partially restores the fast increase of PPARG in both knockdown cells. Together with the results in Fig 6, this result can be interpreted that rosiglitazone, which is soluble in water at low concentrations, can directly access the activating binding pocket of PPARG without needing a cell-internal lipid transport mechanism (Fig 7D). In contrast, fatty acids, which have a much

lower solubility in water, require a lipid transport mechanism to reach PPARG and this transport function requires either FABP4 or FABP5 in these cell systems.

One question is how can FABP4, which is not a transcription factor, increase PPARG expression? Since FABP4 can directly bind to PPARG in the prescence of lipid (Figures 6F and 6G), does this binding stabilize PPARG? To test this, we measured degradation rates of PPARG in the presence of cycloheximide, an inhibitor of protein synthesis (Fig 7E).Neither knockout FABP4 nor overexpression of FABP4 in OP9 cells showed significant differences in PPARG degradation rates, suggesting that FABP4 increases PPARG expression by activating PPARG which then activates transcriptional feedback loops to PPARG. Together, these results provide support for the model depicted in Fig 7F that FABP4 increases PPARG activity by transporting lipids, by binding to PPARG, and by increasing the fraction of PPARG with bound lipids.

## DISCUSSION

Differentiation processes can be described as non-linear systems that have multiple stable states (local attractors) that reflect intermediate states, terminally differentiated states and likely also unwanted stable states without a benefit for the organism. A key question is how cells ensure that they assume the correct cell identity of a specific terminally differentiated state given that other local attractors such as senescence may exist in its vicinity where some or all of the functionality of a cell is lost. Our study considered that one solution to the cell identity problem is to reinforce the differentiation path to a specific differentiated state by using a core component of the differentiated state that not only allows the differentiated cell to properly function but also uses this same factor in a separate regulatory capacity to also initiate the differentiation program and maintain the differentiated state. Our study focused on the question if and how FABP4, one of the most abundant proteins in mature adipocytes that regulates lipid flux, promotes the initiation and commitment to the differentiated state.

When FABP4 is knocked out in mice, there is no decrease in fat mass [14]. But this study also indicates a potential compensatory regulation [15]. In FABP4-knockout mice, FABP5 expression was

massively increased: 40-fold at the mRNA level and 13 to 20-fold at the protein level [14,18]. In support of such a compensatory role, when both FABP4 and FABP5 were knocked out in mice, there was a significant reduction in total body adipose tissue mass both on regular and high-fat diet [31], supporting that FABP4 and FABP5 can compensate for each other. Indeed, we observed the same compensation of FABP5 in FABP4 KO OP9 cells (Fig S1A). FABP5 may have such a compensatory role as it has high sequence similarity to FABP4 and binds to several FAs as well as to hormone sensitive lipase (HSL) with similar affinity and selectivity as FABP4 [32–34]. Nevertheless, these same studies also showed that FABP4/5 deficient precursor cells differentiate well when stimulated with rosiglitazone. Earlier studies also showed that the relative half-maximal increase in FABP4 occurs later than for PPARG.

The overall goal of our study was to test the hypothesis that a core component of a terminal differentiation state can also double-up and function as a regulator to reinforce the differentiation fate. Since FABP4 is a candidate for a factor with such a dual tole, we investigated the role of FABP4 by using simultaneous single-cell analysis of endogenously tagged FABP4 and PPARG to test if and when FABP4 and PPARG regulate each other. We envisioned that this type of analysis can reconcile the seemingly conflicting results in the literature that might be tied to a high variability in the dynamics of FABP4 expression and the possibility that low levels of FABP4 might activate PPARG. By tracking cells and monitoring the master regulator PPARG over time, we showed that the underlying regulatory circuit of the adipocyte differentiation system is characterized by three sequential Phases with DMI mediating a linear increase in PPARG in Phase 1, positive feedback starting to engage at the end of Phase 1, and the bistable switch triggered at the end of Phase 2 when PPARG levels reach a critical threshold where self-amplification takes over and the external input stimulus is not needed any more. We showed that FABP4, and FABP5 if FABP4 is missing, is a necessary slow co-factor needed in OP9 and 3T3-F442A cells to accelerate the build-up of PPARG in Phase 2 to the threshold where differentiation is triggered. Thus, our study suggests that FABP4 has at least three distinct roles in adipocytes: a cell-external role as a mediator released from mature adipocytes to suppress progenitor

and other cell types, and two cell-internal roles: to transport and buffer fatty acids in mature cells during lipolysis, and at very low levels, to act in adipocyte precursor cells as a signaling mediator that transfers fatty acids to PPARG and increase its activity to promote differentiation.

Our study further addressed the question of how FABP4 can regulate PPARG since studies of how FABP4 regulates PPARG have yielded contradictory results. Some studies suggested that FABP4 upregulates PPARG expression and activity in adipocytes [3,9,17] whereas other studies provide evidence that FABP4 suppresses PPARG expression and activity [12,35]. We showed that knocking down or knocking out both FABP4 and FABP5 in OP9 cells and 3t3-F442A results in a significant suppression of adipogenesis. This first appeared to contradict earlier results which showed that WT cells, FABP4/FABP5 KO cells, FABP4/FABP5 KO cells can still effectively differentiate when rosiglitazone was added along with the DMI. Our study shows that these double knockout cells fail to respond to DMI but differentiate in response to rosiglitazone. We also show that FABP4 can directly interact with PPARG and that a mutant deficient in fatty acid binding has increased PPARG affinity without bound fatty acid. Together, these results suggest that rosiglitazone can bind directly to the lipid-binding pocket of PPARG and may therefore bypass the need for FABP4 to bring fatty acids to PPARG. Such a mechanism is plausible as fatty acids have low water solubility while rosiglitazone was developed as a partially water-soluble compound. Together with our knockout, mutant and rescue analysis, we also used live-cell imaging and showed a rapid increase of endogenously tagged PPARG mediated by rosiglitazone. Thus, by mediating direct activation, rosiglitazone can bypass the need for FABP4. Together, our study is consistent with the interpretation that the activity of PPARG is increasingly activated in the second phase of differentiation by FABP4-mediated transport and activation of PPARG by fatty acids, allowing cells to reach the threshold for irreversible differentiation. This supports a dual role of FABP4 to not only mediate buffering and transport functions in the differentiated state, but also control cell identity by driving precursor cells towards irreversible differentiation.

## AUTHOR CONTRIBUTIONS

Z.B., T.H., S.T., E.B., M.L.Z., and M.N.T. designed and carried out the experiments and analyzed data. F.B.K. designed experiments and contributed to discussion. Z.B. and M.N.T. wrote the manuscript with input from all authors.


## ACKNOWLEDGEMENTS

This work was supported by National Institutes of Health RO1-DK101743, RO1-DK106241, P50-GM107615, P30 DK116074, a Stanford BioX Seed Grant, and a Stanford Diabetes Research Center Seed Grant (to M.N.T.), 1F31DK112570-01A1 (to M.L.Z.), DFG Research Fellowship TH2156/1-1 (to S.T.), AHA Fellowship (to E.B.), and by the Department of Veterans Affairs (Office of Research and Development, Medical Research Service) to F.B.K. We thank Tobias Meyer (Stanford University) and members of the Teruel Lab for discussions and critical reading of the manuscript.


## DECLARATION OF INTERESTS

The authors declare no competing interests.

## REFERENCES


1. Kutejova E, Sasai N, Shah A, Gouti M, Briscoe J. Neural Progenitors Adopt Specific Identities by Directly Repressing All Alternative Progenitor Transcriptional Programs. Dev Cell. The Authors; 2016;36: 639–653. doi:10.1016/j.devcel.2016.02.013

2. Ferrell JE. Self-perpetuating states in signal transduction: Positive feedback, double-negative feedback and bistability. Curr Opin Cell Biol. 2002;14: 140–148. doi:10.1016/S0955-0674(02)00314-9

3. Ahrends R, Ota A, Kovary KM, Kudo T, Park BO, Teruel MN. Controlling low rates of cell differentiation through noise and ultrahigh feedback. Science. 2014;344: 1384–9. doi:10.1126/science.1252079

4. Shi Y, Chen J, Karner CM, Long F. Hedgehog signaling activates a positive feedback mechanism involving insulin-like growth factors to induce osteoblast differentiation. Proc Natl Acad Sci U S A. 2015;112: 4678–83. doi:10.1073/pnas.1502301112

5. Ferrell JE, Machleder EM. The biochemical basis of an all-or-none cell fate switch in Xenopus oocytes. Science. 1998;280: 895–898. doi:10.1126/science.280.5365.895

6. Jukam D, Desplan C. Binary fate decisions in differentiating neurons. Curr Opin Neurobiol. 2010;20: 6–13. doi:10.1016/j.conb.2009.11.002

7. Coe NR, Bernlohr DA. Physiological properties and functions of intracellular fatty acid-binding proteins. Biochim Biophys Acta - Lipids Lipid Metab. 1998;1391: 287–306. doi:10.1016/S0005-2760(97)00205-1

8. Jenkins-Kruchten AE, Bennaars-Eiden A, Ross JR, Shen WJ, Kraemer FB, Bernlohr DA. Fatty acid-binding protein-hormone-sensitive lipase interaction: Fatty acid dependence on binding. J Biol Chem. 2003;278: 47636–47643. doi:10.1074/jbc.M307680200

9. Tan N, Shaw NS, Vinckenbosch N, Liu P, Yasmin R, Desvergne B, et al. Selective Cooperation between Fatty Acid Binding Proteins and Peroxisome Proliferator-Activated Receptors in Regulating Transcription. Mol Cell Biol. 2002;22: 5114–5127. doi:10.1128/MCB.22.14.5114

10. Boss M, Kemmerer M, Brune B, Namgaladze D. FABP4 inhibition suppresses PPARgamma activity and VLDL-induced foam cell formation in IL-4-polarized human macrophages. Atherosclerosis. Elsevier Ltd; 2015;240: 424–430. doi:10.1016/j.atherosclerosis.2015.03.042

11. Bahrami-Nejad Z, Zhao ML, Tholen S, Hunerdosse D, Tkach KE, van Schie S, et al. A Transcriptional Circuit Filters Oscillating Circadian Hormonal Inputs to Regulate Fat Cell Differentiation. Cell Metab. Elsevier Inc.; 2018;27: 854-868.e8. doi:10.1016/j.cmet.2018.03.012

12. Garin-Shkolnik T, Rudich A, Hotamisligil GS, Rubinstein M. FABP4 attenuates PPARγ and adipogenesis and is inversely correlated with PPARγ in adipose tissues. Diabetes. 2014;63: 900–911. doi:10.2337/db13-0436

13. Tontonoz P, Hu E, Spiegelman BM. Stimulation of adipogenesis in fibroblasts by PPARgamma2, a lipid-activated transcription factor. Cell. 1994;79: 1147–1156. doi:10.1016/0092-8674(94)90006-X

14. Hotamisligil GS, Johnson RS, Distel RJ, Ellis R, Papaioannou VE, Spiegelman BM. Uncoupling of Obesity from Insulin Resistance Through a Targeted Mutation in aP2, the Adipocyte Fatty Acid Binding Protein. Science. 1996;274: 1377–1379.

15. Shaughnessy S, Smith ER, Kodukula S, Storch J, Fried SK. Adipocyte metabolism in adipocyte

fatty acid binding protein knockout mice (aP2-/-) after short-term high-fat feeding: functional compensation by the keratinocyte [correction of keritinocyte] fatty acid binding protein. Diabetes. 2000;49: 904–11. doi:10.2337/diabetes.49.6.904

16. Ahrends R, Ota A, Kovary KMM, Kudo T, Park BOO, Teruel MNN. Controlling low rates of cell differentiation through noise and ultrahigh feedback. Science. 2014;344: 1384–9. doi:10.1126/science.1252079

17. Ayers SD, Nedrow KL, Gillilan RE, Noy N. Continuous nucleocytoplasmic shuttling underlies transcriptional activation of PPARgamma by FABP4. Biochemistry. 2007;46: 6744–6752. doi:10.1021/bi700047a

18. Coe NR, Simpson MA, Bernlohr DA. Targeted disruption of the adipocyte lipid-binding protein (aP2 protein) gene impairs fat cell lipolysis and increases cellular fatty acid levels. J Lipid Res. 1999;40: 967–972. Available: http://www.ncbi.nlm.nih.gov/pubmed/10224167

19. Djian P, Phillips M, Green H. The activation of specific gene transcription in the adipose conversion of 3T3 cells. J Cell Physiol. 1985;124: 554–556. doi:10.1002/jcp.1041240327

20. Mandrup S, Loftus TM, Macdougald OA, Kuhajda FP, Lane MD. Obese gene expression at in vivo levels by fat pads derived from s.c. implanted 3T3-F442A preadipocytes. Proc Natl Acad Sci U S A. 1997;94: 4300–4305. doi:10.1073/pnas.94.9.4300

21. Lundh M, Pluciñska K, Isidor MS, Petersen PSS, Emanuelli B. Bidirectional manipulation of gene expression in adipocytes using CRISPRa and siRNA. Mol Metab. Elsevier GmbH; 2017;6: 1313–1320. doi:10.1016/j.molmet.2017.07.001

22. Tan N-S, Shaw NS, Vinckenbosch N, Liu P, Yasmin R, Desvergne B, et al. Selective Cooperation between Fatty Acid Binding Proteins and Peroxisome Proliferator-Activated Receptors in Regulating Transcription. Mol Cell Biol. 2002;22: 6318–6318. doi:10.1128/mcb.22.17.6318.2002

23. Cristancho AG, Lazar MA. Forming functional fat: a growing understanding of adipocyte differentiation. Nat Rev Mol Cell Biol. Nature Publishing Group; 2011;12: 722–734. doi:10.1038/nrm3198

24. Rosen ED, Spiegelman BM. What we talk about when we talk about fat. Cell. Elsevier Inc.; 2014;156: 20–44. doi:10.1016/j.cell.2013.12.012

25. Farmer SR. Transcriptional control of adipocyte formation. Cell Metab. 2006;4: 263–73. doi:10.1016/j.cmet.2006.07.001

26. Zhao ML, Rabiee A, Kovary KM, Bahrami-Nejad Z, Taylor B, Teruel MN. A terminal cell differentiation decision based on probabilistic competition between differentiation and mitogenic signals during an extended G1 period. BioRXiv. 2019; https://doi.org/10.1101/632570.

27. Bernlohr DA, Coe NR, LiCata VJ. Fatty acid trafficking in the adipocyte. Semin Cell Dev Biol. 1999;10: 43–9. doi:10.1006/scdb.1998.0271

28. Sha RS, Kane CD, Xu Z, Banaszak LJ, Bernlohr DA. Modulation of ligand binding affinity of the adipocyte lipid-binding protein by selective mutation: Analysis in vitro and in situ. J Biol Chem. 1993;268: 7885–7892.

29. Kim JB, Wright HM, Wright M, Spiegelman BM. ADD1/SREBP1 activates PPARgamma through the production of endogenous ligand. Proc Natl Acad Sci U S A. 1998;95: 4333–4337. doi:10.1073/pnas.95.8.4333

30. Simpson MA, LiCata VJ, Ribarik Coe N, Bernlohr DA. Biochemical and biophysical analysis of the intracellular lipid binding proteins of adipocytes. Mol Cell Biochem. 1999;192: 33–40.

31. Maeda K, Cao H, Kono K, Gorgun CZ, Furuhashi M, Uysal KT, et al. Adipocyte/macrophage fatty acid binding proteins control integrated metabolic responses in obesity and diabetes. Cell Metab. 2005;1: 107–119. doi:10.1016/j.cmet.2004.12.008

32. Furuhashi M, Saitoh S, Shimamoto K, Miura T. Fatty Acid-Binding Protein 4 (FABP4): Pathophysiological Insights and Potent Clinical Biomarker of Metabolic and Cardiovascular Diseases. Clin Med Insights Cardiol. 2014;8: 23–33. doi:10.4137/CMC.S17067.RECEIvED

33. Haunerland NH, Spener F. Fatty acid-binding proteins - Insights from genetic manipulations. Prog Lipid Res. 2004;43: 328–349. doi:10.1016/j.plipres.2004.05.001

34. Hotamisligil GS, Bernlohr DA. Metabolic functions of FABPs—mechanisms and therapeutic implications. Nat Rev Endocrinol. 2015;11: 592–605. doi:10.1038/nrendo.2015.122

35. Kralisch S, Klöting N, Ebert T, Kern M, Hoffmann A, Krause K, et al. Circulating adipocyte fatty acid-binding protein induces insulin resistance in mice *in vivo*. Obesity. 2015;23: 1007–1013. doi:10.1002/oby.21057

36. Wolins NE, Quaynor BK, Skinner JR, Tzekov A, Park C, Choi K, et al. OP9 mouse stromal cells rapidly differentiate into adipocytes: characterization of a useful new model of adipogenesis. J Lipid Res. 2006;47: 450–60. doi:10.1194/jlr.D500037-JLR200

37. Green H, Kehinde O. An established preadipose cell line and its differentation in culture II. Factors affecting the adipose conversion. Cell. 1975;5: 19–27.

38. Mandrup S, Loftus TM, MacDougald OA, Kuhajda FP, Lane MD. Obese gene expression at in vivo levels by fat pads derived from s.c. implanted 3T3-F442A preadipocytes. Proc Natl Acad Sci U S A. 1997;94: 4300–4305. doi:10.1073/pnas.94.9.4300

39. Ran FA, Hsu PD, Wright J, Agarwala V, Scott D, Zhang F. Genome engineering using the CRISPR-Cas9 system. Nat Protoc. 2013;8: 2281–308. doi:10.1038/nprot.2013.143

40. Nagoshi E, Saini C, Bauer C, Laroche T, Naef F, Schibler U. Circadian gene expression in individual fibroblasts: Cell-autonomous and self-sustained oscillators pass time to daughter cells. Cell. 2004;119: 693–705. doi:10.1016/j.cell.2004.11.015

41. Ran FA, Hsu PD, Lin CY, Gootenberg JS, Konermann S, Trevino AE, et al. Double nicking by RNA-guided CRISPR cas9 for enhanced genome editing specificity. Cell. Elsevier; 2013;154: 1380–1389. doi:10.1016/j.cell.2013.08.021

42. Shcherbo D, Murphy CS, Ermakova G V, Solovieva E a, Chepurnykh T V, Shcheglov AS, et al. Far-red fluorescent tags for protein imaging in living tissues. Biochem J. 2009;418: 567–574. doi:10.1042/BJ20081949

43. Konermann S, Brigham MD, Trevino AE, Hsu PD, Heidenreich M, Cong L, et al. Optical control of mammalian endogenous transcription and epigenetic states. Nature. Nature Publishing Group; 2013;500: 472–6. doi:10.1038/nature12466

## FIGURE LEGENDS

**Figure 1: Preadipocytes without FABP4 are defective in differentiation in vitro and in vivo.**
(A) Schematic of proposed cell-identity positive feedback.
(B) Description of assay used to quantitate adipogenesis. Cells were plated into 96-well plates. 24 hours post transfection, the cells were induced to differentiate by addition of the adipogenic cocktail DMI (1 μM dexamethesone, 250 μM IBMX, 1.75 nM insulin) for 48 hours, followed by 48 hours in just 1.75 nM insulin.
(C) Validation of FABP4 knockout using CRISPR-mediated genome editing. Immunoblotting of undifferentiated (Day 0) and differentiated (Day 4) OP9-cells in which FABP4 was knocked out. Control-KO are cells that were transfected and sorted at the same time but that did not harbor FABP4 knockout. β-actin was used as loading control.
(D) Validation of the FABP5 knockdown efficiency using single-cell immunocytochemistry.
(E) Knockout of FABP4 AND knockdown of FABP5 in OP9 preadipocyte cells reduces PPARG expresssion and adipogenesis as assessed by the assay described in (B). Single cell immunofluorescence of wild type OP9 vs FABP4 cells: Bar plots represent mean +/– s.e.m. from 3 technical replicates. All data shown are representative of 3 independent experiments.
(F) Immunoblotting for FABP4 and FABP5 in differentiated 3T3-F442A WT, FABP4- KO, FABP5 KO and double knockout of FABP4 and FABP5 cells. β-actin was used as loading control.
(G, H) Knockout of FABP4 reduces 3T3-F442A adipocyte differentiation. Knocking out both FABP4 and FABP5 together reduces diffentiation even further. Cells were grown to 2 days post-confluence and were induced to differentiate into adipocytes with insulin. At day 6 post-induction, the extent of adipogenesis was assessed by immunocytochemistry o PPARG. Bar plots represent mean +/- SEM from three technical replicates with approximately 1000 cells per replicate. Data shown is representative of three independent experiments.
(I) De novo fat formation model used to analyze developed fat pads from subcutaneously-implanted 3T3-F442A preadipocytes. To induce de novo fat pad formation, 3T3-F442A preadipocytes (3 x 107) were grown to near confluency, re-suspended in PBS and were injected subcutaneously in the sternum of 8-week old male immune-deficient mice. Fat pads that developed from the implanted preadipocytes were excised, fixed, sectioned, and stained with hematoxylin and eosin at 4 weeks after implantation
(J) The weight of the fat pads extracted 4 weeks after injection show that there is no significant fat formation in FABP4-KO, FABP5-KO, and DBKO 3T3-F442A cells whereas wildtype-KO 3T3-F442A cells robustly formed fat. Error bars show Mean + SD; unpaired t-test: *** $p < 0.001$.

**Fig 2: Increasing FABP4 expression using CRISPRa in a mesenchymal stem cell (MSC) line increases PPARG expression and adipogenesis.**
(A) C3 Figure 2: Increasing FABP4 expression by direct overexpression or by CRISPRa increases PPARG expression and adipogenesis.
(A) Overexpression of YFP(control) or FABP4 (YFP-FABP4) in OP9 cells resulted in maximal differentiation.
(B) Generation of FABP4-KO preadipocyte OP9 cells in which YFP(control) or YFP-FABP4 could be overexpressed in a doxycycline-inducible manner
(C) Overexpression of YFP-FABP4 in FABP4-KO cells rescued the differentiation capacity.
(D) Schematic of the CRISPRa assay used to increase FABP4 expression in a C3H10T1/2 (MSC)

cells.
(E) Differentiation assay as in Figure 1A, but now carried out in C3H10T1/2 cells. Single cell immunofluorescence of control(EV) vs overexpression of FABP4 cells: Bar plots represents mean +/– s.e.m. from 3 technical replicates. All data shown are representative of 3 independent experiments.

**Figure 3. Kinetic analysis of endogeneous FABP4 and PPARG protein levels during adipogenesis.**
(A) Endogenous FABP4 was tagged with mKate2 (RFP) in the citrine-PPARG cells. Images show live dual-tagged OP9 cells differentiated for 4 days into adipocytes by applying the standard adipogenic cocktail (DMI) for 2 days followed by 2 days in media with just insulin. Scale bar, 10 µM. See also Figures S1 and S2.
(B) Timecourse analysis of the dual-tagged cells described in (A).
(C) Changes in PPARG and FABP4 expression measured in the same cell over the timecourse of adipogenesis. Timecourses from 4 representative cells are shown.
(D) Timecourses of citrine-PPARG/mKate2-FABP4 cells during application of a 48-hr adipogenic (DMI) stimulus. Plotted lines are population median traces with shaded regions representing 25$^{th}$ and 75$^{th}$ percentiles of approximately 700 cells per condition, representative of 3 independent experiments.
(E) Bar plots of the increase in PPARG and FABP4 relative to the maximal levels of the respective proteins reached during the timecourse.

**Figure 4. FABP4 is not needed early in adipogenesis, but is needed later to reach the threshold level at which cells irreversible commit to differentiate.**
(A) Schematic of the relationship between CEBPB, CEBPA, FABP4, and PPARG to control adipogenesis.
(B) Single cell PPARG timecourses colored according to their bimodal level of PPARG at 96 hours.
(C) Examples of single-cell 96-hour time courses of changes in PPARG expression of OP9 cells stimulated as in (B)
(D) PPARG timecourses comparing the average of ~700 cells that will differentiate (red) and the average of ~400 cells that will not differentiate (blue) from the same experiment. As shown by the dotted black lines, the abundance of PPARG gradually increases at a relatively constant slope for about 24 hours before the increase in PPARG begins to accelerate.
(E) The slope of PPARG at each timepoint was calculated by using a linear fit to 8-hour segments of the PPARG abundance trajectory (+/- 4 hours). A feedback engagement point is clearly apparent and occurs many hours before a cell will cross the threshold where differentiation is triggered. The same dataset was used in (D) and (E) and is representative of five independent experiments.
(F-H) Live cell imaging of citrine-PPARG cells following transfection with CEBPA-targeted or control(YFP) siRNA shows that knockdown of CEBPA, a main feedback partner of PPARG, results in loss of the feedback engagement point. Cells were stimulated to differentiate with the standard 48-hour DMI protocol described in Figure 1b. Plotted lines are population median traces with shaded regions representing 25th and 75th percentiles of approximately 700 cells per condition.
(I) The PPARG abundance and slope values from (D) and (E) were used to calculate a threshold by at 44 hours, a timepoint before DMI was removed. A clear threshold that predicts whether the same cell will be differentiated at 96 hours can be seen for both PPARG abundance and slope.

**Figure 5: The early, small increase in FABP4 occurs in parallel with increasing PPARG expression and before cells reach the threshold to differentiate**

(A) Timecourses of 494 dual-tagged cells were binned according to their PPARG level at 48 hours, and the traces in each bin were averaged. Plot shows representative averaged timecourses to show a range of differentiation outcomes. The data show is representative of 5 independent experiments.

(B) Zoomed-in region of (A) showing a direct comparison of the gradual increases in PPARG and FABP4 before both get self-amplified when cells reach the engagement point.

(C) The red and black binned traces from (A) are plotted on a log2 y-axis in order to better see the threshold. If the PPARG level in a cell goes above the threshold, that cell will continue on to differentiate even if the adipogenic stimulus is removed. If PPARG level do not reach the threshold before the differentiation stimulus is removed, that cell will drop back to the undifferentiated state.

(D) Schematic illustrating where FABP4, a slow feedback partner of PPARG, is highly active to control the critical middle phase of differentiation (Phase 2) during which cells commit irreversibly to differentiate. During Phase 1, the master regulator PPARG slowly increases to the feedback engagement point, primarily driven by the external DMI stimulus. During Phase 2, both external stimulation and internal self-amplification are needed to increase PPARG levels up to the threshold. In Phase 3, which begins after the Threshold is reached, the cell trajectory becomes independent of input stimulus, and a further increase can be driven by internal self-amplification alone until the terminal differentiation state is reached. The observed drop in PPARG level is due to loss of the input stimulus before PPARG levels once again increase due to positive feedback to PPARG. The long delay before the threshold is reached suggests that this system may filter out short pulses of differentiation stimuli.

**Figure 6. The lipid-binding activity of FABP4 is needed to increase PPARG expression and induce adipogenesis.**

(A) Generation of stable cell lines in which YFP-FABP4(WT), non fatty-acid binding mutant YFP-FABP4$_{R126Q}$, or YFP(control) can beoverexpressed in a doxycycline-inducible manner in the FABP4-KO OP9 cell line.

(B) Overexpression of YFP(control) or wildtype FABP4 (YFP-FABP4) in OP9 cells resulted in maximal differentiation. In contrast, overexpression of YFP-FABP4$_{R126Q}$, a non-fatty acid binding mutant of FABP4, resulted in reduced differentiation compared to control.

(C) Overexpression of YFP-FABP4WT in FABP4-KO cells rescued the differentiation capacity. In contrast, overexpression of YFP(control) or YFP-FABP4$_{R126Q}$, a non-fatty acid binding mutant of FABP4, in the FABP4-KO cells resulted in no differentiation.

(D) Generation of a reporter for PPARG activity. The construct, 3XPPRE-mKate2-NLS-PEST, was stably expressed in FABP4-KO OP9 cells.

(E) WT FABP4 enhances PPARG activation in a ligand-dependent fashion. Activation of PPARG in a ligand-dependent fashion is greatly reduced when the FABP4 mutant (R126Q) is overexpressed. Stable OP9 cells were made co-expressing 3XPPRE-mKate2-NLS-PEST and either doxycycline-inducible-YFP-FABP4(WT) or doxycycline-inducible-YFP-FABP4$_{R126Q}$ mutant. FABP4 or FABP4 (R126Q) expression was induced or kept basal by the addition of doxycycline or fatty acid-free BSA (control), respectively, and different doses of linoleic acid or fatty acid-free BSA (control) were added to the cells.

(F) To assess PPARG interaction with FABP4, co-IPs on total cell lysate were performed using GFP

nanobody or IgG(control) antibodies in FABP4 KO cells with doxycycline-inducible-YFP-FABP4 or doxycycline-inducible-YFP-FABP4$_{R126Q}$ mutant. It was immunoblotted for FABP4 and PPARG (n = 2 experiments). At t=0 hours, cells were treated with both linoleic acid (100 μM) and doxycycline (1ug/ml). Co-IP's on the total cell lysates were performed at day two.
(G) Co-IP's were carried out as in (F) at different time points during differentiation. Media containing linoleic acid was refreshed every day.
(H) Schematic of how FABP4 brings fatty acid ligands to activate PPARG.

**Figure 7. Rosiglitazone, a PPARG agonist which binds to the same binding pocket in PPARG as fatty acid, bypasses the need for FABP4 upregulating PPARG expression during adipogenesis.**
(A) Knockout of FABP4 and FABP5 impairs adipogenesis in 3T3-FF42A preadipocyte cells induced to differentiate by the standard protocol of adding insulin.
(B-C) The addition of 1 μM Rosiglitazone rescues the loss of adipogenesis in FABP4-KO, FABP5-KO, and DBKO 3T3-F442A cells. Percent of differentiated cells was quantitated as in Figure 1G.
(A-B) Scale bar is 30 mm.
(D) Addition of Rosiglitazone rescues the loss of adipogenesis in FABP4-KO OP9 cells or FABP4-KO OP9 cells transfected with FABP5 siRNA. Cells were induced to differentiate by addition of DMI. 24 hours post transfection, the cells were induced to differentiate with different differentiation cocktail (DMI = 1 uM dexamethasone, 250 uM IBMX, 1.75 nM insulin or 1 μM Rosiglitazone) for 48 hours, followed by 48 hours media with insulin. DMI was used to indirectly activate PPARG, and Rosiglitazone was used to directly activate PPARG. Percent of differentiated cells was quantitated as in Figure 1B.
(E) Live cell imaging of citrine-PPARG and mKate2-FABP4 cells following transfection with FABP4 and FABP5-targeted or control (YFP) siRNA shows that knockdown of FABP4 and FABP5, results in loss of differentiation. However, this phenotype was partially rescued by rosiglitazone, which directly activated PPARG. Cells were stimulated to differentiate by adding DMI.
(F) FABP4KO-YFP-FABP4 or FABP4KO-YFP(control) cells were stimulated with DMI for 48 hr before treated with cyclohexamide and fixed at the indicated time points, immunofluorescence was performed to measure PPARG protein levels.The shaded region represents the 95th confidence bounds on the fitted coefficients. Values enclosed in parentheses show lower and upper bounds on the estimated half-life derived from the 95% confidence bounds.
(G) Schematic showing how rosiglitazone bypasses the need for FABP4 in activating PPARG.

## SUPPLEMENTARY FIGURE LEGENDS

**Fig S1. Schematic of how dual tagged citrine(YFP)-PPARG and mKate2(RFP)-FABP4 OP9 preadipocyte cell lines were generated.**

**Fig S2. Validation of mKate2-FABP4 tagging.**

## CONTACT FOR REAGENT AND RESOURCE SHARING

Further information and requests for reagents may be directed to, and will be fulfilled by the corresponding author, Dr. Mary N. Teruel (mteruel@stanford.edu).

## EXPERIMENTAL MODEL DETAILS

OP9 mouse stromal cell line [36]

3T3-F442A mouse preadipocyte cell [37]

Immune-deficient mouse-J:NU (Jackson Labs, Cat #007860)

## METHOD DETAILS

### Cell culture and differentiation

OP9 cells were cultured according to previously published protocols [3,36]. OP9 cells were cultured in 20% Fetal Bovine Serum (FBS) in growth media consisting of MEM-α (Invitrogen, #12561) and 100 units/mL Penicillin, 100µg/mL Streptomycin, and 292 µg/mL L-glutamate (Invitrogen, # 10378-016). 3T3-F442A cells were cultured in 10% bovine calf serum in growth media consisting of DMEM, 2 mM L-glutamine, 100 U/ml penicillin, and 100 U/ml streptomycin. To induce differentiation of OP9 cells, confluent cells were treated with a differentiation medium containing a commonly used DMI (dexamethasone/IBMX/insulin) stimulus to initiate adipogenesis. DMI consists of dexamethasone (dex), a synthetic glucocorticoid; 3-isobutyl-1-methylxanthine (IBMX), an inhibitor of phosphodiesterase that increases cAMP levels; and insulin. Applying the DMI stimulus consisted of replacing the media on the cells with growth media plus 10% FBS, 0.25 mM IBMX (Sigma Cat # 7018), 1 µM dexamethasone (Sigma Cat #D1756), and 1.75 nM insulin (Sigma Cat # I6634) (Stimulus I). Two days after initiating differentiation, Stimulus I was removed from the cells and was replaced with Stimulus II consisting of growth media plus 10% FBS and 1.75 nM insulin for two more days. As noted in some experiments, rosiglitazone (Cayman, USA) was added to the media to result in a final concentration of 1 µM.

3T3-F442A preadipocytes were grown and differentiated according to established protocols[19]. Briefly, 3T3-F442 cells were grown in in growth media consisting of DMEM (100U/ml) supplemented with 10% bovine serum (BS) and 1% penicillin/streptomycin (PS). Cells were passaged when pre-confluent. For differentiation, preadipocytes were grown to confluency on plates coated with collagen-1 (Advanced BioMatrix, 5005). When confluent, differentiation was induced by changing media to growth media + insulin (5$\mu$g/ml) for four days. After day 4, the media was replaced with just growth media. This latter media was replaced every two days on the cells until the cells were fully differentiated, which occurred typically around day 10 after induction of differentiation.

**Oil Red O staining**

To determine lipid accumulation 3T3-F442A preadipocytes were differentiated for 10 days and stained with Oil Red O. The cells were washed with phosphate-buffered saline (PBS) and fixed using 4% paraformaldehyde (PFA) for 1h. Cells were washed using double-distilled $H_2O$ and incubated with the filtered Oil Red O solution (Cat #O0625, Sigma) for 1h. Cells were washed twice with $ddH_2O$ and analyzed by bright-field microscopy.

***De novo* adipogenesis *in vivo***

To induce *de novo* fat pad formation, preadipocytes were grown to near confluency and resuspended in PBS. 3 x $10^7$ preadipocytes were injected subcutaneously at the sternum of 8-week old male athymic mice (Cat. #007850, Jackson Laboratory) as described previously [38]. After 4 weeks, mice were anesthetized with isoflurane and sacrificed by cervical dislocation. Fat pads derived from the implanted cells were excised and weighed.

**Generation of FABP4-KO, FABP5-KO, and DBKO cells:**

The CRISPR-Cas9 constructs targeting FABP4 and FABP5 were generated based on a previously described protocol [39]. Briefly, different guide RNAs targeting FABP4 or FABP5 were designed

(crispr.mit.edu) and oligos including the targeting sequences were annealed and cloned into pSpCas9n(BB)-2A-GFP (PX461; Addgene #48140), used for targeting FABP4, or pSpCas9(BB)-2A-miRFP670 (Addgene #91854), used for targeting FABP5. Constructs were transfected into 3T3-F442A preadipocytes or OP9 preadipocytes via electroporation using the Amaxa Cell Line Nucleofector Kit V (Lonza, Cologne, Germany). Afterwards cells were grown two days in DMEM, 10% BS and 100 U/ml penicillin/streptomycin for 3T3-F442A or for OP9 MEM with L-glutamine, 20% FBS, and 100 U/ml penicillin/streptomycin. FACS-sorting was performed to select for construct marker (GFP and/or iRFP expression), and cells were seeded in 96-well plates (1 cell/well) to analyze them for FABP4 and/or FABP5 expression. Single cells that did not harbor any FABP4-KO were expanded to obtain WT(control) clones. Successfully transfected cells were sorted for positive cells and assayed for loss of FABP4, FABP5 or both proteins.

**Generation of stable cell lines with doxycycline-inducible shRNA targeting FABP4 or control:** The construct for inducible overexpression of shRNA used the PB-CMV-MCS-EF1α-Puro vector (Systems Biosciences, Palo Alto, CA) as the backbone in a Gibson assembly reaction. The vector was cut with SpeI and BstXI restriction enzymes. A Tet Response Element (TRE) was cloned upstream of a minimal CMV promoter, followed by the coding sequence of far red fluorescent protein iRFP670 and a shRNA destination site with two BstXI cut sites. Additionally, ubiquitin promoter was placed upstream of the coding sequence for blasticidin resistance protein Blasticidin-S deaminase (BSD), linked to reverse tetracycline-controlled transactivator (rtTA) by a GS linker and a T2A self-cleaving peptide. Next, gene-specific shRNAs were introduced by cutting this construct with BstXI and ligating it with an insert, obtained by alignment of two oligonucleotides which formed sticky ends complementary to the BstXI cut sites. The shRNA sequences used are provided in the Supplementary Table. To obtain stable OP9 lines with inducible shRNA expression, cells were co-transfected with an shRNA vector and a Piggy Bac transposase-containing vector using Lipofectamine 2000 and later underwent selection in the presence of blasticidin S.

**Generation of stable, doxycycline-inducible FABP4 overexpression cell lines (in mouse OP9 cells):** The Lenti-X Tet-On Advanced lentiviral inducible expression system (Clontech Laboratories, Mountain View, CA) was used to generate a doxcycline-inducible protein expression system in our stable OP9 FABP4-KO cell line. This system needs two elements: 1) the Regulator Vector (pLVX-Tet-On Advanced) and the Response Vector (pLVX-Tight). Our FABP4-KO OP9 cells were co-transduced with pLVX-Tet-On Advanced and either pLVX-Tight-YFP-FABP4(WT), pLVX-Tight-YFP-FABP4 (R126Q) or pLVX-Tight-YFP(control) lentiviruses. Cells were then grown in media containing neomycin and blasticidin S to select clones expressing the two constructs, and FACS was used to further enrich for YFP-positive cells.

To carry out experiments, the stable OP9 FABP4-KO cells with inducible YFP-wild type FABP4, YFP-FABP4 (R126Q) or YFP were plated 10K at day -1. Cells were grown in MEM with L-glutamine, 20% FBS, and 100 U/ml penicillin/streptomycin. At day 0, the cells were treated with doxycycline 1ug/ml and adipogenic cocktail in MEM with L-glutamine, 10% FBS, and 100 U/ml penicillin/streptomycin.

**Generation of live-cell sensor for PPARG activity: 3XPPRE-mKate2(RFP)-NLS-PEST**

To create the PPRE: mKate2(RFP)-NLS-PEST construct in a PiggyBac delivery system, an in-house Gibson cloning reaction mix was used. Blasticidin resistance was previously introduced in place of puromycin in the PB-CMV-MCS-EF1α-Puro vector (System Biosciences), which was then linearized using SfiI/XbaI restriction enzyme digestion to obtain the backbone. Phusion High-Fidelity DNA Polymerase (New England Biolabs) was used to amplify the PPRE sequence from the PPRE X3-TK-luc construct (Addgene, #1015), the mKate2 sequence from the pDONR P2R-P3-mKate2 construct (Addgene, #48345), and the NLS-PEST sequence from the RevErb-Venus-NLS-PEST [40]. The final plasmid was transfected into OP9 cells using Lipofectamine 2000 (Thermo Fisher Scientific). Cells

were selected using 10 µg/ml blasticidin (Invivogen) for at least 7 days, and single-cell clones were obtained by FACS.

**Generation of stable OP9 cell lines to measure PPARG activity (FABP4-KO-PPRE)**

Stable OP9 FABP4 knockout cells containing inducible YFP-WT-FABP4 or YFP-FABP4 (R126Q) were transfected with mKate2(RFP)-NLS-PEST, a sensor for PPARG activity. These cells were plated at a density of 8000 cells per well into 96-well plates at Day -1. Cells were grown in MEM with L-glutamine, 20% FBS, and 100 U/ml penicillin/streptomycin. At Day 0, the cells were treated with doxycycline (1ug/ml). To determine the effect of linoleic acid on PPARG activity, linoleic acid (LA, Sigma-Aldrich L1012) was first dissolved in 100% ethanol to a concentration of 1M, mixed with 10% fatty acid-free BSA (Sigma-Aldrich A8806) in MEM medium, and then incubated at 37°C for 4 hours to form LA-BSA complexes at a final concentration of 1mM LA. Then the 1 mM mixture of LA-BSA complexes was diluted 10-fold in MEM to a stock concentration of 100 µM. This stock concentration was then further diluted with additional MEM to make serial dilutions that were applied to cells for 24 hours.

**Workflow used to generate single cell colonies with endogenously tagged PPARG and FABP4 (mouse OP9 cells, Fig S3):**

To carry out CRISPR genome editing to generate FABP4-mkate2, we used the "double nickase" system which uses two different guide RNAs that create adjacent and opposing nicks in the DNA at the site of insertion [11,41]. To carry out double-nickase genome-editing, two different targeting sequences (sgRNA) directed to the FABP4 locus were designed as described above and inserted into the guide RNA site of two plasmids, pX335-U6-Chimeric_BBCBh-hSpCas9n (pX335) (Addgene plasmid #42335) encoding the SpCas9 D10A nickase. Oligonucleotide duplexes encoding each desired targeting sequence were ligated into the BbsI cut sites of px335. Construction and design of the donor template were carried out based on Bahrami-Nejad et al, 2018. Previously, CRISPR-mediated genome editing was used to tag the N-terminus of endogenous PPARG in OP9 cells. These

cells were next used to tag the C-terminus of FABP4 with mKate2, a bright red fluorescent protein [42]. The DNA repair template to promote homology directed repair (HDR)-mediated insertion of the fluorescent protein (mkate2) was constructed by inserting the cDNA of mkate2-3xGly flanked by two 800 bp homology arms into the entry vector backbone pENTR1a (Addgene Plasmid #17398). The pENTR1a backbone vector was digested with EcoRI-HF and BamHI-HF (NEB), and assembled together with three DNA fragments by using Gibson assembly.

**Immunoblotting**

For SDS-PAGE, 20 ug protein per lane was used. Proteins were detected with anti-PPARG (1:1000, Santa Cruz Biotechnology, sc-7273), anti-FABP4 (1:1000 R&D Systems, AF1443), anti-FABP5 (1:1000 Cell Signaling, 5174), anti-GFP (1:1000 Abcam, ab290) and anti-tRFP (1:1000 Evrogen EVN-AB233-C100).

**Co-Immunoprecipitation (Co-IP)**

Twenty-four hours before the start of the experiment, stable FABP4-KO OP9 cells with either inducible YFP, YFP-WT-FABP4 or YFP-FABP4 (R126Q) were treated with doxycycline (1ug/ml) and in alpha-MEM with L-glutamine, 10% FBS, and 100 U/ml penicillin/streptomycin. At t=0 hours, cells were treated with both linoleic acid (100 µM) and doxycycline (1ug/ml). Co-IP's on the total cell lysates or on subcellular fractions (nuclear and cytoplasmic) were performed at different timepoints using anti-GFP $V_HH$ coupled to magnetic agarose beads (GFP-Trap_MA, Chromotek) or, as a control, IgG (Chromotek), following the manufacturer's instructions. The same amount of protein was used for each IP, and the protein concentration was measured using a BSA kit.

**ChIP-qPCR**

Chromatin immunoprecipitation (ChIP) was performed using ExactaChIP reagents (R & D Systems) according to the manufacturer's instructions with slight modifications. At Day -1, stable FABP4-KO

OP9 cells harboring inducible YFP(control), YFP-FABP4(WT), or YFP-FABP4(R126Q) were treated with 1ug/ml doxycycline and with adipogenic cocktail in MEM with L-glutamine, 10% FBS, and 100 U/ml penicillin/streptomycin. At Day 0, cells were treated with both 100 µM linoleic acid and 1ug/ml doxycycline. At Day 2, 20 × $10^6$ cells were fixed with 1% formaldehyde in PBS to cross-link protein-DNA complexes. The formaldehyde was quenched by addition of glycine to a final concentration of 0.125 M. Cells were lysed with 500 µl of lysis buffer (R&D Systems). Chromatin was sonicated with a Bioruptor (Diagenode) in order to generate fragment genomic DNA with a size of 0.5–2 kb. The fragmented genomic DNA was incubated overnight at 4°C with anti-PPARG (1:1000, Santa Cruz Biotechnology, sc-7273) or the negative control IgG (5415; Cell signaling). Protein G Dynal magnetic beads were added to the ChIP reactions and incubated for two hours at 4 degC. The magnetic beads were washed, and chromatin was eluted with a chelating resin solution (R&D Systems), followed by DNA purification. Quantitative PCR was carried out using GoTaq qPCR Master Mix (Promega), according to the manufacturer's instructions.

**FABP4 Gain-of-Function in pre-adipocytes via CRISPRa SAM**

Murine mesenchymal C3H10T1/2 cells stably expressing the CRISPRa-SAM complex were used for gain of function experiments following a previously established protocol [21]. Briefly, to make the sable cell line, the CRISPRa-SAM components (dCas9-VP64 and MS2-P65-HSF1) were delivered in lentiviruses by plasmid co-transfection of C3H10T1/2 cells. The resulting cell line (C3H10T1/2-CRISPRa-SAM) can be used for activation of endogenous genes via chemical transfection with a single guide RNA (sgRNA)-containing plasmid. C3H10T1/2-CRISPRa-SAM cells were maintained in high glucose-DMEM media containing FBS (10%), Penicillin-streptomycin (1%), and blasticidin (2.5 ug/ml) and hygromycin (200 ug/ml) to ensure a retained dCas9-SaM expression. sgRNA sequences targeting FABP4 promoter regions were designed using the 'SAM genome engineering online tool' (http://sam.genomeengineering.org/database/), and annealed and ligated into the backbone vector following the original protocol [43]. Correct insertion was verified by sequencing of plasmids. The

sequence used was FABP4 (NM_024406.3) CATACAGGGTCTGGTCATGA. Cell transfections were performed as previously described [21]. Briefly, for gene expression analysis (RT-qPCR), 300,000 cells were seeded per well into a 12-well plate (Day -3), transfected at confluence (Day -2) using Mirus TransIT-X2 transfection reagent (3ul per well; Mirus Bio LLC, US) and 250 ng plasmid DNA (either empty vector or FABP4 sgRNA). For staining experiments, 2000 cells were seeded per well into a 96-well Costar Plastic plate. The day after, the cells were transfected with a total of 50 ng sgRNA per well using 0.25 µl TransIT-X2 reagent per well. Two days following transfection at Day 0, all cells received either only DMI or DMI and Rosiglitazone (1 uM) to induce adipogenesis. The non-stimulated cells were used as a control. At Day 2, the media was replaced with media containing only insulin. At Day 4, the cells were either fixed for protein staining or lysed for mRNA analysis

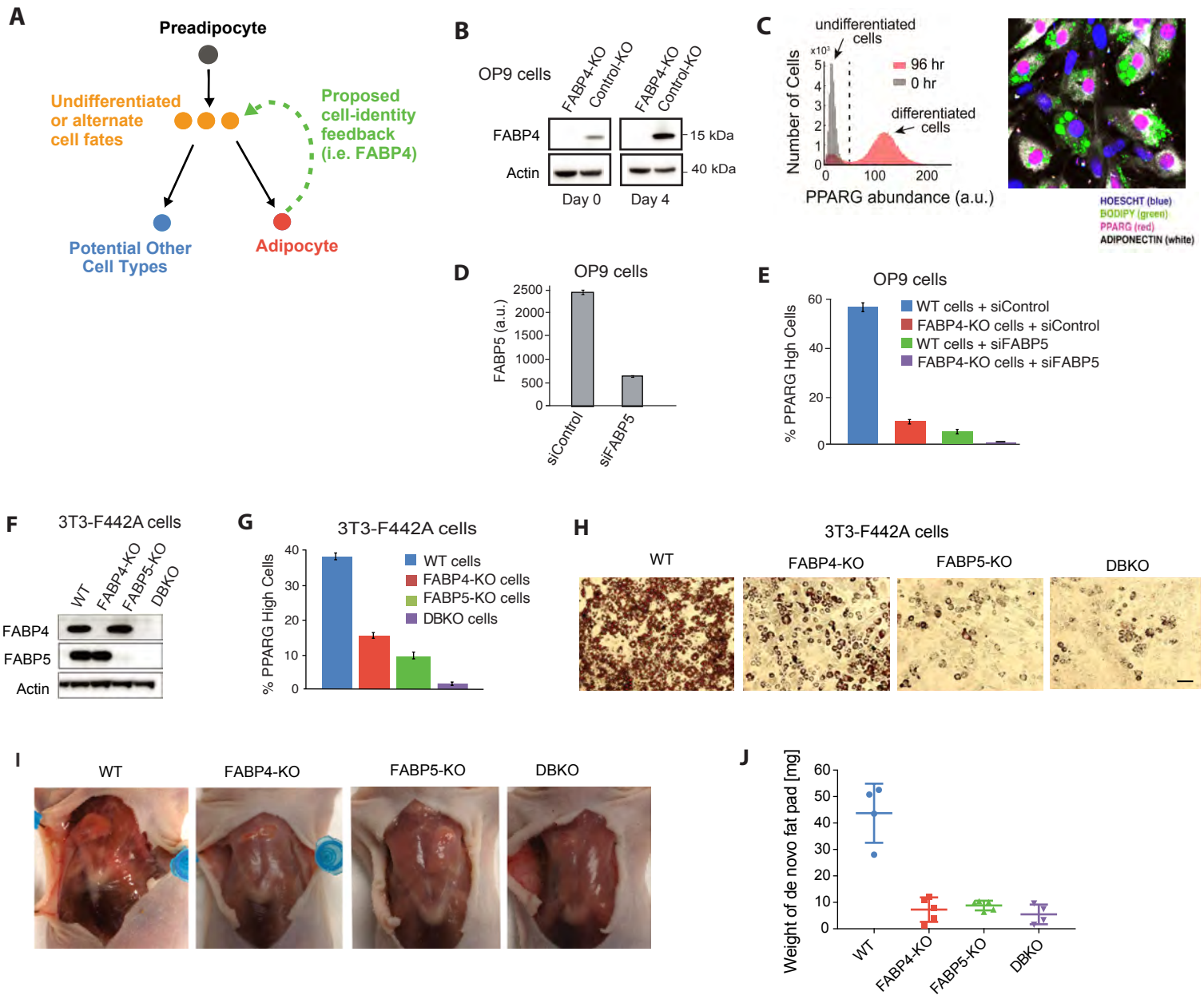


**Figure 1: Preadipocytes without FABP4 are defective in differentiation in vitro and in vivo.**
(A) Schematic of proposed cell-identity positive feedback.
(B) Description of assay used to quantitate adipogenesis.
(C) Knockdown of FABP4 AND FABP5 in OP9 preadipocyte cells reduces differentiation as assessed differentiation assay described in (A).
(D) Immunoblotting of undifferentiated (Day 0) and differentiated (Day 4) OP9-cells in which FABP4 was knocked out using CRISPR-mediated genome editing. Control-KO are cells that were transfected and sorted at the same time but that did not harbor FABP4 knockout. β-actin was used as loading control.
(E) Differentiation assay as in (B), but now carried out in FABP4-KO cells. Single cell immunofluorescence of wild type OP9 vs knockout FABP4 cells: Bar plots in (D, E) represents mean +/– s.e.m. from 3 technical replicates. All data shown are representative of 3 independent experiments. siRNA-meditated knockdown of FABP5 in FABP4-KO cells suppresses differentiation. OP9 and FABP4-KO cells were plated into 96-well plate and transfected with siRNA targeting FABP5 or control (YFP). 24 hours post transfection, the cells were induced to differentiate with differentiation cocktail (DMI = 1 μM dexamethasone, 250 μM IBMX, 1.75 nM insulin) for 48-hours, followed by 48 hours media with insulin.
(F) Immunoblotting for FABP4 and FABP5 in differentiated 3T3-F442A WT, FABP4- KO, FABP5 KO and double knockout of FABP4 and FABP5 cells. β-actin was used as loading control.
(G, H) Knockout of FABP4 reduces 3T3-F442A adipocyte differentiation. Knocking out both FABP4 and FABP5 together reduces differentiation even further. Cells were grown to 2 days post-confluence and were induced to differentiate into adipocytes with insulin. At day 6 post-induction, the extent of adipogenesis was assessed by immunocytochemistry to PPARG. Bar plots represent mean +/- SEM from three technical ‘ replicates with approximately 1000 cells per replicate. Data shown is representative of three independent experiments.
(I) De novo fat formation model used to analyze developed fat pads from subcutaneously-implanted 3T3-F442A preadipocytes (ref). To induce de novo fat pad formation, 3T3-F442A preadipocytes ($3 \times 10^7$) were grown to near confluency, re-suspended in PBS and were injected subcutaneously in the sternum of 8-week old male immune-deficient mice. Fat pads that developed from the implanted preadipocytes were excised, fixed, sectioned, and stained with hematoxylin and eosin at 4 weeks after implantation.
(J) The weight of the fat pads extracted 4 weeks after injection show that there is no significant fat formation in FABP4-KO and double FABP4/FABP5-KO 3T3-F442A cells whereas wildtype-KO 3T3-F442A cells robustly formed fat. Error bars show Mean + SD; unpaired t-test: *** $p < 0.001$.

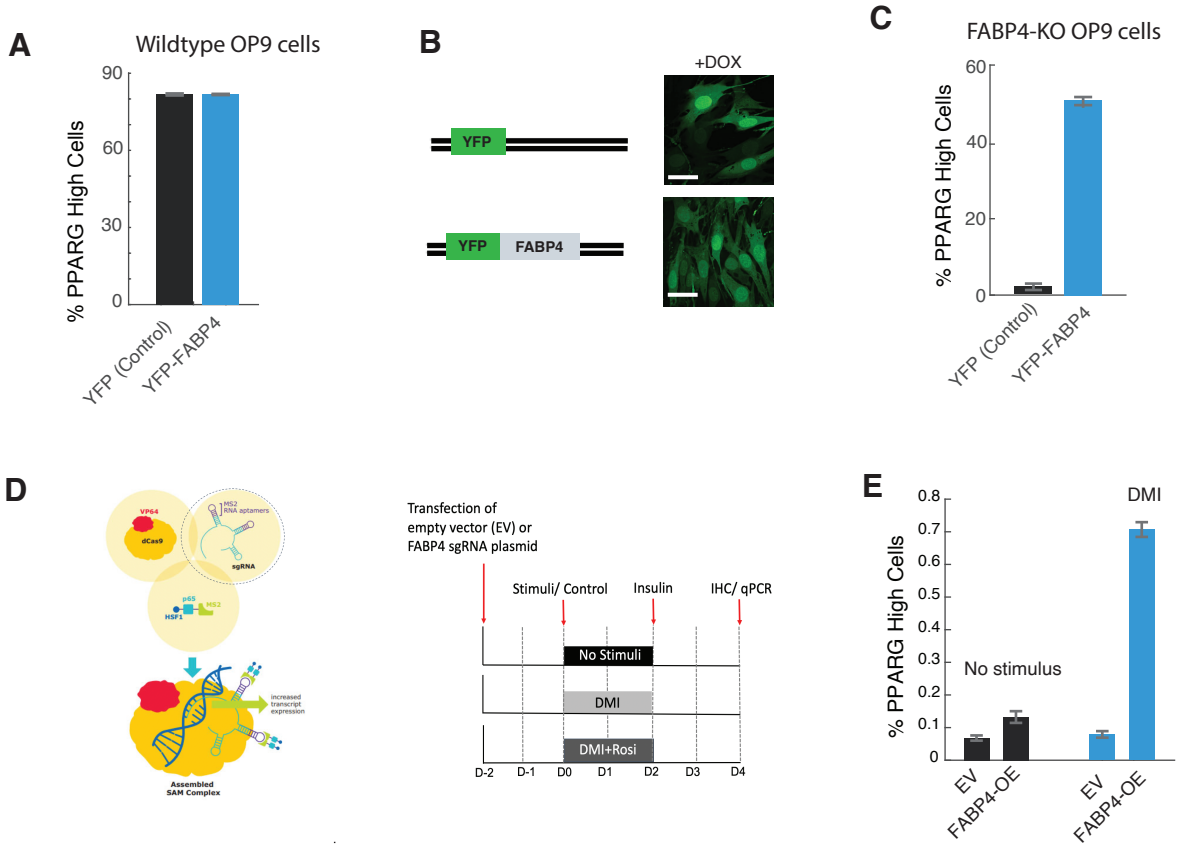


**Figure 2: Increasing FABP4 expression by direct overexpression or by CRISPRa increases PPARG expression and adipogenesis.**

(A) Overexpression of YFP(control) or FABP4 (YFP-FABP4) in OP9 cells resulted in maximal differentiation.

(B) Generation of FABP4-KO preadipocyte OP9 cells in which YFP(control) or YFP-FABP4 could be overexpressed in a doxycycline-inducible manner

(C) Overexpression of YFP-FABP4 in FABP4-KO cells rescued the differentiation capacity.

(D) Schematic of the CRISPRa assay used to increase FABP4 expression in a C3H10T1/2 (MSC) cells.

(E) Differentiation assay as in Figure 1A, but now carried out in C3H10T1/2 cells. Single cell immunofluorescence of control(EV) vs overexpression of FABP4 cells: Bar plots represents mean +/– s.e.m. from 3 technical replicates. All data shown are representative of 3 independent experiments.

.

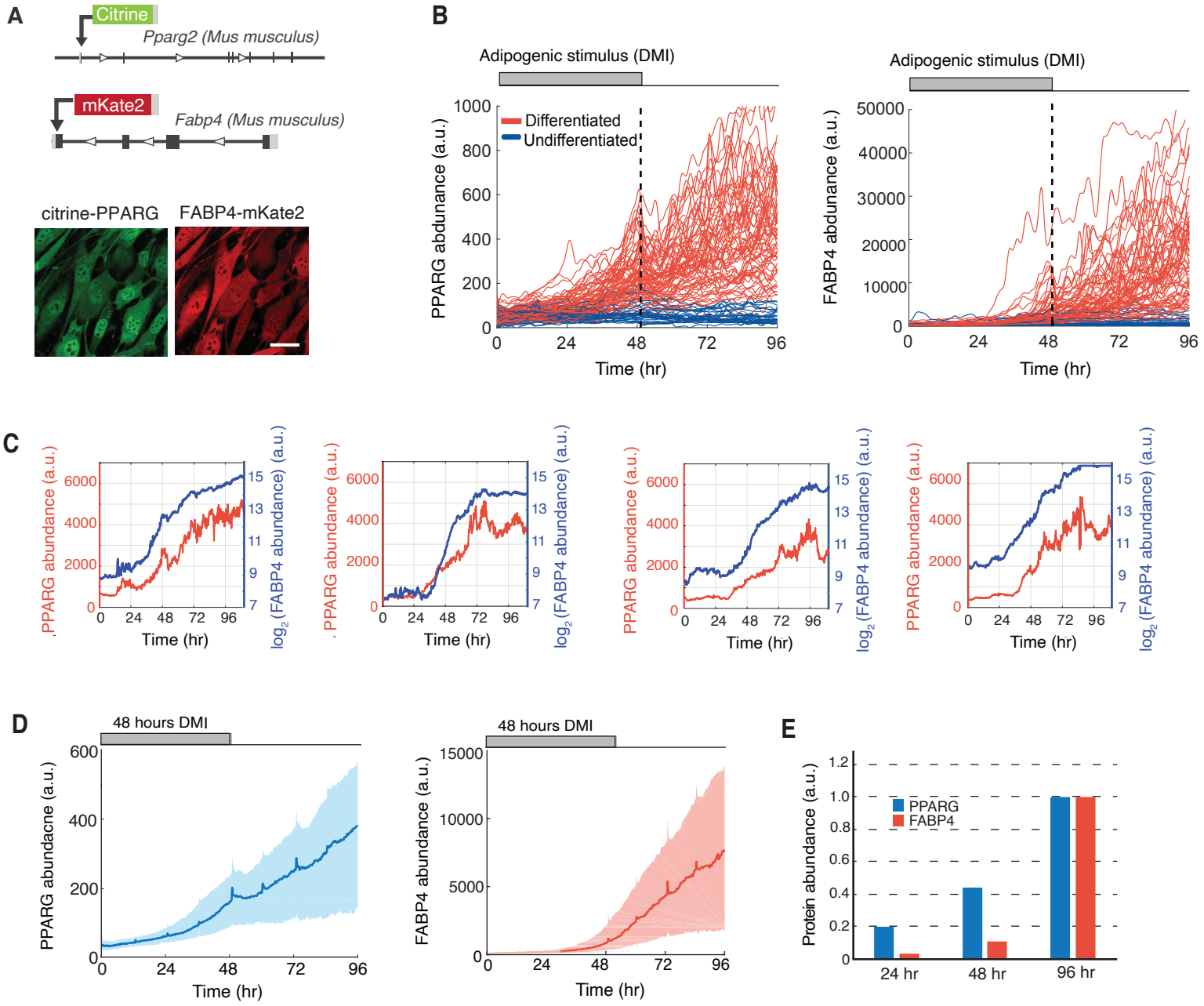


**Figure 3. Kinetic analysis of endogeneous FABP4 and PPARG protein levels during adipogenesis.**
(A) Endogenous FABP4 was tagged with mKate2 (RFP) in the citrine-PPARG cells. Images show live dual-tagged OP9 cells differentiated for 4 days into adipocytes by applying the standard adipogenic cocktail (DMI) for 2 days followed by 2 days in media with just insulin. Scale bar, 10 μM. See also Figures S1 and S2.
(B) Timecourse analysis of the dual-tagged cells described in (A).
(C) Changes in PPARG and FABP4 expression measured in the same cell over the timecourse of adipogenesis. Timecourses from 4 representative cells are shown.
(D) Timecourses of citrine-PPARG/mKate2-FABP4 cells during application of a 48-hr adipogenic (DMI) stimulus. Plotted lines are population median traces with shaded regions representing 25th and 75th percentiles of approximately 700 cells per condition, representative of 3 independent experiments.
(E) Bar plots of the increase in PPARG and FABP4 relative to the maximal levels of the respective proteins reached during the timecourse.

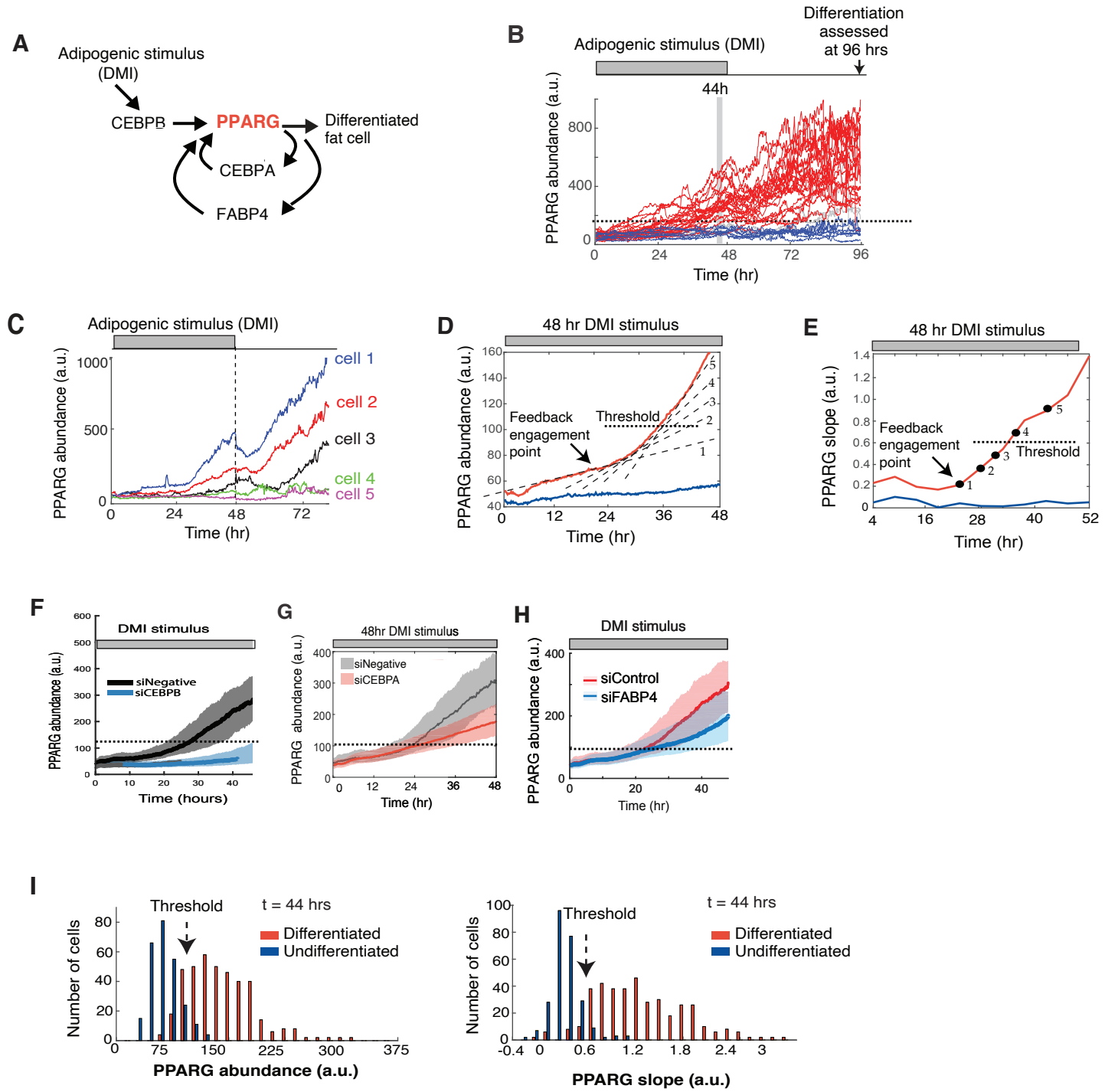


**Figure 4. FABP4 is not needed early in adipogenesis, but is needed later to reach the threshold level at which cells irreversible commit to differentiate.**

(A) Schematic of the relationship between CEBPB, CEBPA, FABP4, and PPARG to control adipogenesis.

(B) Single cell PPARG timecourses colored according to their bimodal level of PPARG at 96 hours.

(C) Examples of single-cell 96-hour time courses of changes in PPARG expression of OP9 cells stimulated as in (B)

(D) PPARG timecourses comparing the average of ~700 cells that will differentiate (red) and the average of ~400 cells that will not differentiate (blue) from the same experiment. As shown by the dotted black lines, the abundance of PPARG gradually increases at a relatively constant slope for about 24 hours before the increase in PPARG begins to accelerate.

(E) The slope of PPARG at each timepoint was calculated by using a linear fit to 8-hour segments of the PPARG abundance trajectory (+/- 4 hours). A feedback engagement point is clearly apparent and occurs many hours before a cell will cross the threshold where differentiation is triggered. The same dataset was used in (D) and (E) and is representative of five independent experiments.

(F-H) Live cell imaging of citrine-PPARG cells following transfection with CEBPA-targeted or control(YFP) siRNA shows that knockdown of CEBPA, a main feedback partner of PPARG, results in loss of the feedback engagement point. Cells were stimulated to differentiate with the standard 48-hour DMI protocol described in Figure 1b. Plotted lines are population median traces with shaded regions representing 25th and 75th percentiles of approximately 700 cells per condition.

(I) The PPARG abundance and slope values from (D) and (E) were used to calculate a threshold by at 44 hours, a timepoint before DMI was removed. A clear threshold that predicts whether the same cell will be differentiated at 96 hours can be seen for both PPARG abundance and slope.

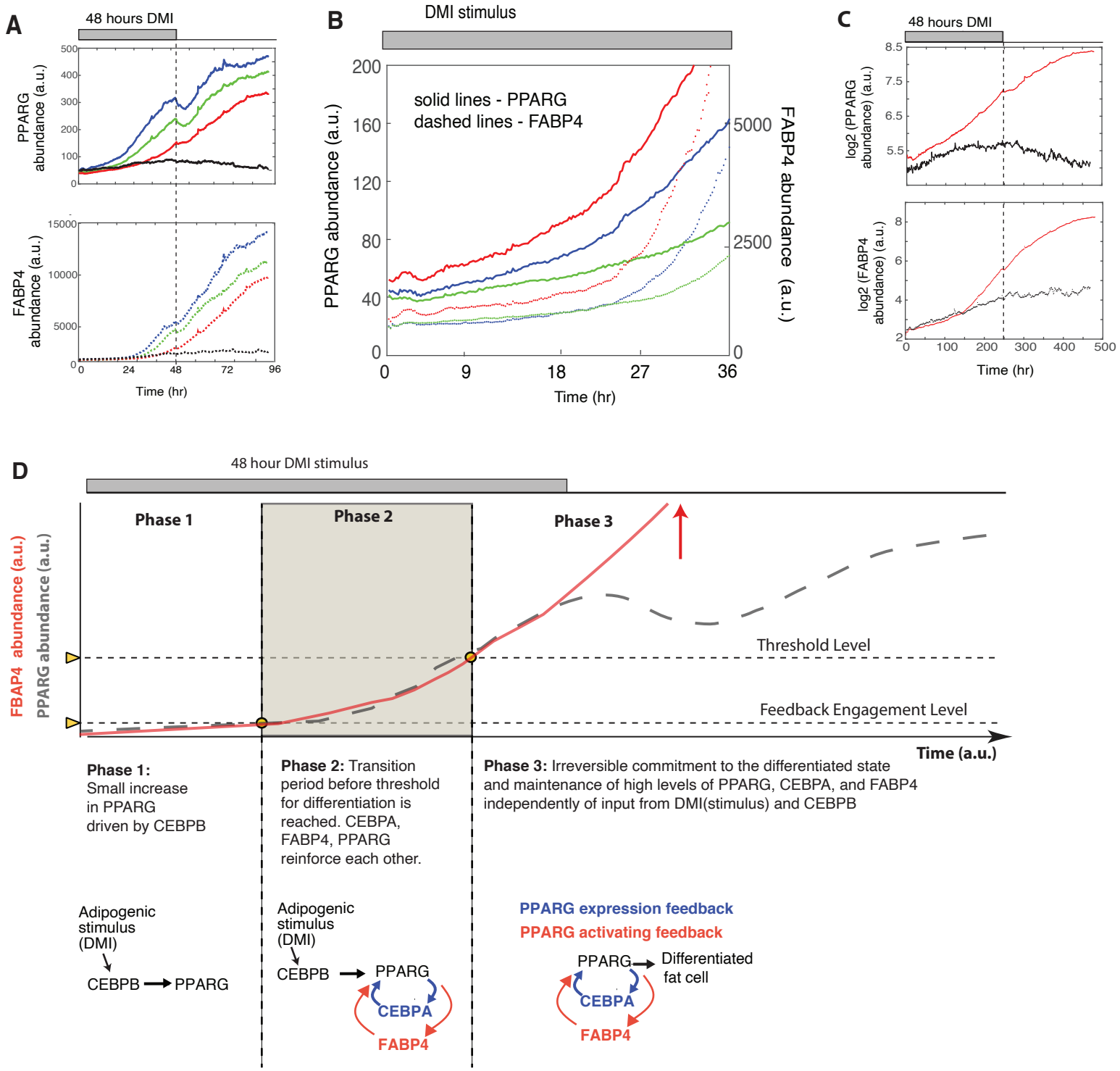


**Figure 5. The early, small increase in FABP4 occurs in parallel with increasing PPARG expression and before cells reach the threshold to differentiate.**

(A) Timecourses of 494 dual-tagged cells were binned according to their PPARG level at 48 hours, and the traces in each bin were averaged. Plot shows representative averaged timecourses to show a range of differentiation outcomes. The data show is representative of 5 independent experiments.

(B) Zoomed-in region of (A) showing a direct comparison of the gradual increases in PPARG and FABP4 before both get self-amplified when cells reach the engagement point.

(C) The red and black binned traces from (A) are plotted on a log2 y-axis in order to better see the threshold. If the PPARG level in a cell goes above the threshold, that cell will continue on to differentiate even if the adipogenic stimulus is removed. If PPARG level do not reach the threshold before the differentiation stimulus is removed, that cell will drop back to the undifferentiated state.

(D) Schematic of a three-phase model of adipogenesis: FABP4 controls the critical middle phase (Phase 2) during which cells commit to the differentiated state.

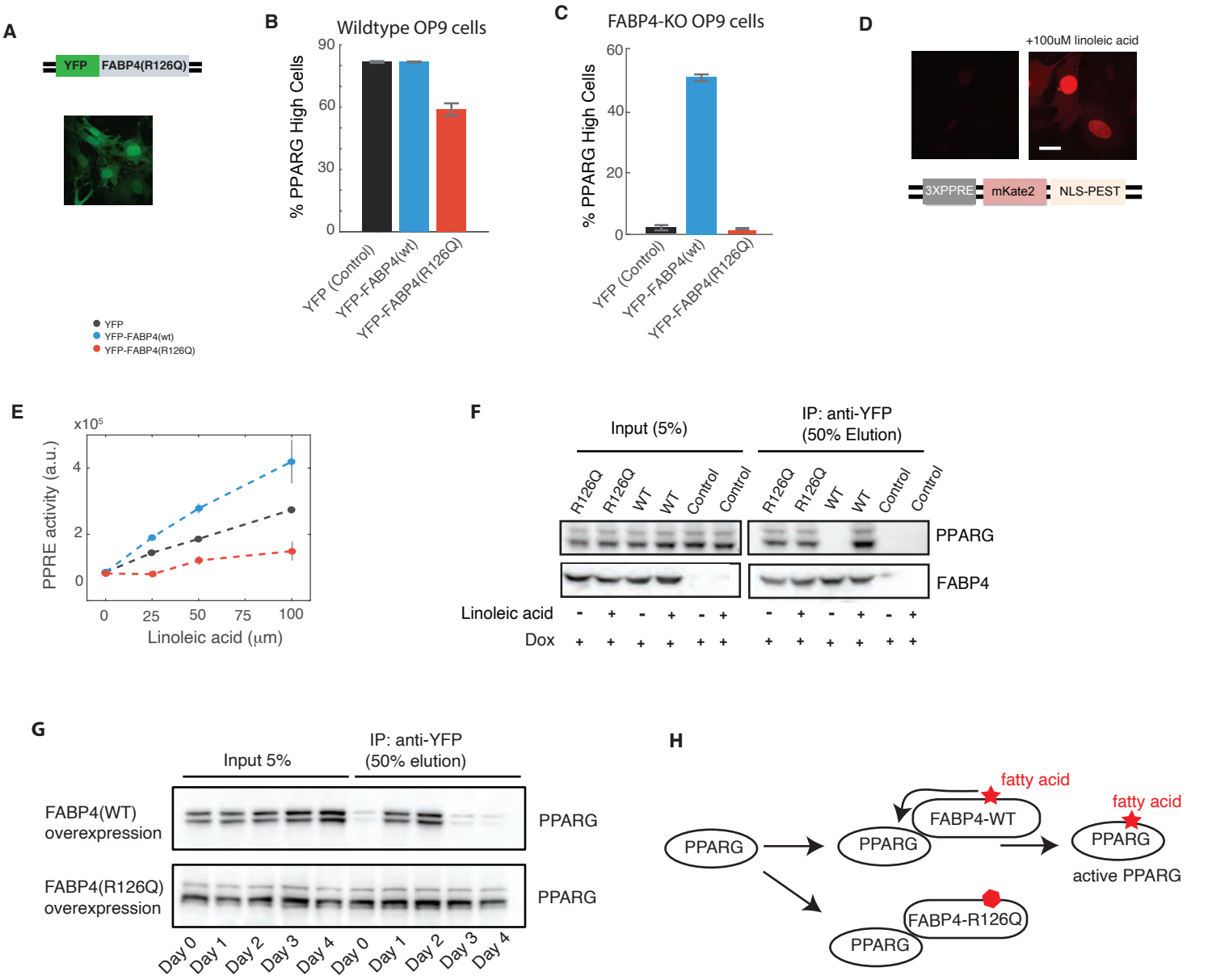


**Figure 6. The lipid-binding activity of FABP4 is needed to increase PPARG expression and induce adipogenesis.**
(A) Generation of stable cell lines in which YFP-FABP4WT, non fatty-acid binding mutant YFP-FABP4R126Q, or YFP(control) can be overexpressed in a doxycycline-inducible manner in the FABP4-KO OP9 cell line.
(B) Overexpression of YFP(control) or wildtype FABP4 (YFP-FABP4WT) in OP9 cells resulted in maximal differentiation. In contrast, overexpression of YFP-FABP4R126Q, a non-fatty acid binding mutant of FABP4, resulted in reduced differentiation compared to control.
(C) Overexpression of YFP-FABP4WT in FABP4-KO cells rescued the differentiation capacity. In contrast, overexpression of YFP(control) or YFP-FABP4R126Q, a non-fatty acid binding mutant of FABP4, in the FABP4-KO cells resulted in no differentiation.
(D) Generation of a reporter for PPARG activity. The construct, 3XPPRE-mKate2-NLS-PEST, was stably expressed in FABP4-KO OP9 cells.
(E) WT FABP4 enhances PPARG activation in a ligand-dependent fashion. Activation of PPARG in a ligand-dependent fashion is greatly reduced when the FABP4 mutant (R126Q) is overexpressed. Stable OP9 cells were made co-expressing 3XPPRE-mKate2-NLS-PEST and either doxycycline-inducible-YFP-FABP4WT or doxycycline-inducible-YFP-FABP4R126Q mutant. FABP4 or FABP4 (R126Q) expression was induced or kept basal by the addition of doxycycline or fatty acid-free BSA (control), respectively, and different doses of linoleic acid or fatty acid-free BSA (control) were added to the cells.
(F) To assess PPARG interaction with FABP4, co-IPs on total cell lysate were performed using GFP nanobody or IgG(control) antibodies in FABP4 KO cells with doxycycline-inducible-YFP-FABP4 or doxycycline-inducible-YFP-FABP4R126Q mutant. It was immunoblotted for FABP4 and PPARG (n = 2 experiments). At t=0 hours, cells were treated with both linoleic acid (100 μM) and doxycycline (1ug/ml). Co-IP's on the total cell lysates were performed at day two.
(G) Co-IP's were carried out as in (F) at different time points during differentiation. Media containing linoleic acid were refreshed every day.
(H) Schematic of how FABP4 brings fatty acid ligands to activate PPARG.

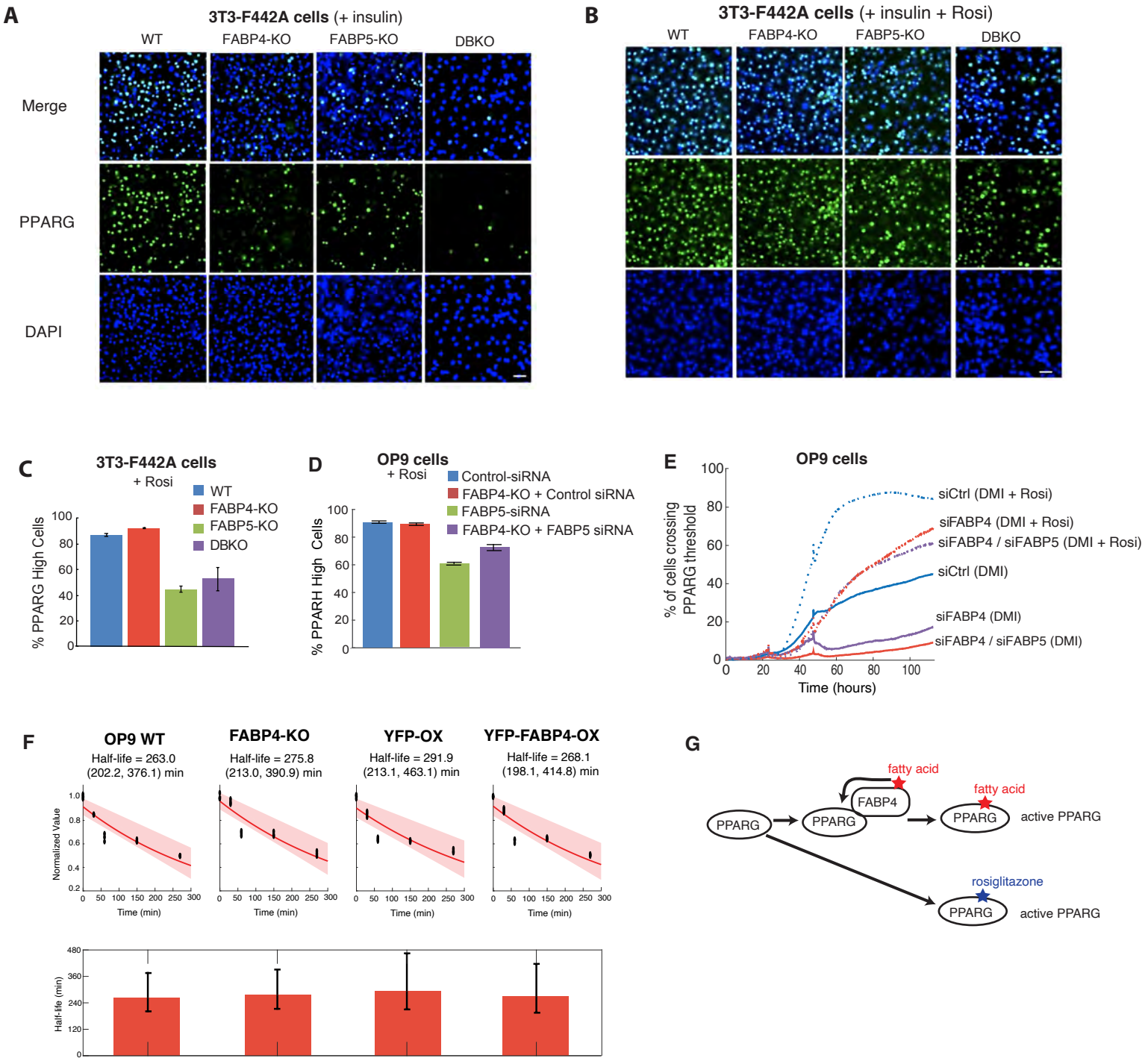


**Figure 7. Rosiglitazone, a PPARG agonist which binds to the same binding pocket in PPARG as fatty acid, bypasses the need for FABP4 upregulating PPARG expression during adipogenesis.**

(A) Knockout of FABP4 and FABP5 impairs adipogenesis in 3T3-FF42A preadipocyte cells induced to differentiate by the standard protocol of adding insulin.

(B-C) The addition of 1 μM Rosiglitazone rescues the loss of adipogenesis in FABP4-KO, FABP5-KO, and DBKO 3T3-F442A cells. Percent of differentiated cells was quantiated as in Figure 1G.

(A-B) Scale bar is 30 μm.

(D) Addition of Rosiglitazone rescues the loss of adipogenesis in FABP4-KO OP9 cells or FABP4-KO OP9 cells transfected with FABP5 siRNA. Cells were induced to differentiate by addition of DMI. 24 hours post transfection, the cells were induced to differentiate with different differentiation cocktail (DMI = 1 uM dexamethasone, 250 uM IBMX, 1.75 nM insulin or 1 μM Rosiglitazone) for 48h ours, followed by 48 hours media with insulin. DMI was used to indirectly activate PPARG, and Rosiglitazone was used to directly activate PPARG. Percent of differentiated cells was quantiated as in Figure 1B.

(E) Live cell imaging of citrine-PPARG and mKate2-FABP4 cells following transfection with FABP4 and FABP5-targeted or control (YFP) siRNA shows that knockdown of FABP4 and FABP5, results in loss of differentiation. However, this phenotype was partially rescued by rosiglitazone, which directly activated PPARG. Cells were stimulated to differentiate by adding DMI.

(F) Cyclohexamide experiments to measure the degradation of PPARG in the presence of FABP4 and lipids.

(G) Schematic showing how rosiglitazone bypasses the need for FABP4 in activating PPARG.